Available online at www.sciencedirect.com

ScienceDirect

Journal of Magnesium and Alloys 9 (2021) 1–20

www.elsevier.com/locate/jma

Review

Recent developments and applications on high-performance cast magnesium rare-earth alloys

Guohua Wu[a,*], Cunlong Wang[b,*], Ming Sun[c], Wenjiang Ding[a]

[a] National Engineering Research Center of Light Alloy Net Forming and State Key Laboratory of Metal Matrix Composites, Shanghai Jiao Tong University, Shanghai 200240, China

[b] School of Materials Science and Engineering, Jiangsu University, Zhenjiang 212013, Jiangsu Province, China

[c] School of Materials Science and Engineering, University of Shanghai for Science and Technology, Shanghai 200093, China

Received 19 March 2020; received in revised form 5 June 2020; accepted 8 June 2020

Available online 26 November 2020

Abstract

During the past decades, with the increasing demands in lightweight structural materials, Mg alloys with low density and high performance have been extensively investigated and partly applied in some industries. Especially when rare earth (RE) elements are added as major alloying elements to Mg alloys, the alloy strength and creep resistance are greatly improved, which have promoted several series of Mg-RE alloys. This paper reviews the progress and developments of high-performance Mg-RE alloys in recent years with emphasis on cast alloys. The main contents include the alloy design, melt purification, grain refinement, castability, novel liquid casting and semisolid forming approaches, and the industrial applications or trials made of Mg-RE alloys. The review will provide insights for future developments of new alloys, techniques and applications of Mg alloys.

Keywords: Magnesium alloys; Rare-earth elements; High-performance; Developments; Applications; Cast.

1. Introduction

The research and application of Mg alloys have been put into engineering practices for a long time since World War II, when aircrafts and missiles simply took advantages of Mg's lightweight. However, the level of strength and creep resistance was not satisfactory until RE-containing Mg alloys were developed in the late 1990s. With the coming of the 21st century, various types of Mg-RE series alloys have been developed since Rocklin's [1] first summarization of the mechanical performance of Mg-RE binary alloys. In recent years, new Mg-RE series alloys have received considerable researches due to their low densities, high strengths and creep resistances, good ignition proof ability and corrosion resistance.

Quite contrary to the traditional Mg-Al series alloys, alloying with REs in Mg alloys brings several scientific and industrial problems into reality. For examples, the design strategy of the Mg-RE alloy is more complicated, which employs various strengthening mechanisms especially precipitation strengthening. The melt purification of Mg-RE alloys has extra problem of RE loss due to the chemical activities of REs. Grain refinement of Mg-RE alloys is easier through the addition of Mg-Zr master alloy, but the settling of Zr particles causes the waste. Moreover, the commonly used die casting technique for Mg-Al alloy is not applicable to Mg-RE alloys because it cannot exert the heat treatable potential, which has promoted new fabrication methods. In addition, although the use of RE increases the cost of Mg alloys, the applications of Mg-RE alloys in some key areas especially the aerospace and defense areas have shown their irreplaceable advantages.

* Corresponding authors.

E-mail addresses: ghwu@sjtu.edu.cn (G. Wu), cunlongw@gmail.com (C. Wang).

https://doi.org/10.1016/j.jma.2020.06.021

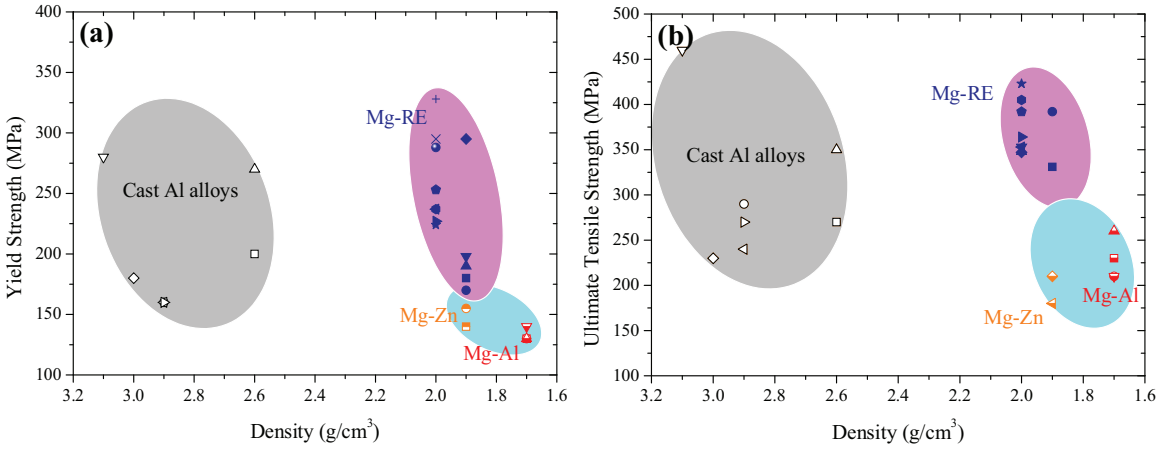

Fig. 1. Comparative illustrations showing the (a) yield strength and (b) ultimate tensile strength as a function of density for T6 heat-treated as-cast Al, Mg-Al, Mg-Zn and Mg-RE series alloys. Note that the data for Al, Mg-Al and Mg-Zn alloys are extracted from [3] and [4], and the data for Mg-RE are mainly based on Table 1 and 2.

Casting is the most fundamental technique for fabricating Mg alloy. A high quality of Mg casting usually includes the factors of melt cleanliness, castability, defect removal, and uniformities in microstructures, grain size and properties etc. Much related work has already been done on the casting Mg-RE alloys, since Mg-RE alloys are the most promising high-performance Mg alloys. It is also expected that the use of Mg-RE alloys will continue to be increased in the next few decades. Therefore, the present paper will summarize noteworthy aspects related to the casting technique of Mg-RE alloys and applications of castings as follows:

(i) recent developments of cast Mg-RE alloys with emphasis on Mg-Gd and Mg-Y alloys;

(ii) melt purification methods and grain refinement techniques for Mg-RE alloys;

(iii) precision liquid metal processing and semisolid forming techniques developed specifically for Mg-RE alloys;

(iv) some real applications of Mg-RE in industries.

This review provides the researchers and engineers with an overall understanding of current developments in high performance Mg-RE cast alloys and new insights into future developments. In addition, the development in Mg-RE wrought alloys can be referred to a recent review by Zhang et al. [2].

2. Development of high-performance MG-RE alloys

Rare earth elements (REs) are generally classified into two groups, namely the light REs and heavy REs. The light REs are elements from La to Eu in the cerium group and heavy REs are elements from Gd to Lu in yttrium group. Due to similar atomic structure and chemical behaviors, Sc and Y are two special cases that have always been classified into the light and heavy REs, respectively. Several Mg-RE system alloys, for instance, the Mg-Gd, Mg-Y, Mg-Nd, Mg-Dy, Mg-Sm and so on have been developed. The developed high-performance Mg-RE alloys have shown relatively higher mechanical properties and comparable densities to conventional Mg-Al or Mg-Zn series alloys, and relatively lower densities and comparable strengths to cast Al alloys. A schematic illustration on the YS and UTS as a function of density for light metals were shown in Fig. 1. However, the Mg-Gd and Mg-Y alloys became the most studied ones due to their strong aging hardening abilities and potentials for real applications. Thus, this section will mainly focus on Mg-Gd and Mg-Y alloys.

2.1. Mg-Gd based alloys

The solute limit of Gd in Mg is ~23.5% at 548 °C (all the compositional percentage are weight percent other than specified), and it can decrease to less than 3% at 200 °C, thus the precipitation strengthening effect from Gd is highly significant. In binary Mg-Gd system or ternary Mg-Gd-X (x = Y [5–10], Sm [11,12], Nd [13], Zn [6,14–20], Ag [21–23], etc.) system, a prominent hardness increase can always be made in peak-aged states when Gd content is approximately 10%, and it is much higher than conventional Mg-Al alloys. A typical age hardening response of Mg-10Gd-3Y alloy at 200 °C is comparatively shown with commercialized WE54 alloy and AZ91D alloy in Fig. 2 [5].

The precipitation sequence of binary Mg-Gd alloys and some ternary or quaternary Mg-Gd-REs system alloys is revealed to be:

S.S.S.S. (Super saturated solid solution) → ordered *G.P.* zones → β'' ($D0_{19}$, Mg_3Gd) → β' (cbco, Mg_7Gd) → β_1 (fcc, Mg_3Gd) → β (fcc, Mg_5Gd) [24].

The peak hardness can be attributed to the precipitation of β' phase with nanoscale and dense distribution, which is a metastable precipitate nucleated at the $(11\bar{2}0)$ lattice plane (prismatic plane, as shown in Fig. 3) and show a coherent interface with the Mg matrix. Thus, a series of β' strengthened alloys were developed and showed relatively excellent room temperature strength and heat resistance. The long been researched Mg-10Gd-3Y-0.5Zr series alloys has been reported to show a yield strength (YS) of 220~240 MPa, ultimate tensile strength (UTS) of 340~380 MPa and elongation to failure (E_f) of 2~4%, and other developed Mg-Gd-RE alloys

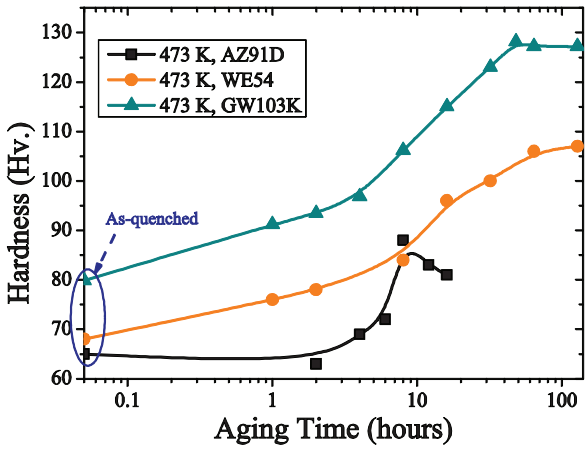

Fig. 2. Comparison of age hardening responses between typical Mg-RE alloy and conventional AZ91D alloy during iso-thermal aging treatment at 200 °C [5].

such as Mg-Gd-Sm [12], Mg-Gd-Nd [13] alloys and quaternary Mg-Gd-Y-Nd alloys [25,26] also show comparative strengths (Note that the addition of Zr only contributes to grain refinement which will be discussed in Section 3.3.1).

Alloying with the third element in Mg-Gd system, the precipitation sequence would be quite different. In the Mg-Gd-Zn system, apart from the aforementioned precipitation sequence in prismatic plane of Mg matrix, a precipitation sequence can also be found in the basal plane of Mg matrix as follows:

S.S.S.S. $\rightarrow \gamma''$ (*hcp*, $Mg_{70}Gd_{15}Zn_{15}$) $\rightarrow \gamma'$ (*hcp*, Mg-GdZn) $\rightarrow \gamma$ (*hcp*, $Mg_{12}GdZn$).

The strengthening effect of β' and γ'' precipitates (as shown in Fig. 3) together with the long period ordered stacking (LPSO, please find details in Section 2.2) phases consequently lead to the development of Mg-Gd-(RE)-Zn alloys. For instance, the Mg-17.4Gd-1.1Zn-0.6Zr alloy can achieve a YS of 278 MPa and UTS of 405 MPa [15]. Similarly, in the Mg-Gd-Ag system, the reported highest strength of YS 328 MPa and UTS 423 MPa can be achieved in the Mg-15.6Gd-1.8Ag-0.4Zr alloy under peak-aged condition. The strength contribution to the final yield strength can mainly be attributed to the co-precipitation of prismatic β' and basal γ'' precipitates. The room temperature tensile strengths of recently developed Mg-Gd based alloys prepared by various casting methods and heat treatment procedures are listed in detail in Table 1.

2.2. Mg-Y based alloys

Before Y was chosen as the major alloying element, QE22 (Mg-2.5%Ag-2.1%RE-0.6%Zr) alloy developed by Magnesium Elektron Ltd. had long been used in aerospace such as aircraft engine intermediate compressor casing and generator housings [28]. The presence of RE (or Th, but Th with radioactivity) and Ag improved elevated temperature strength of Mg alloy. However, QE22 has higher cost and worse corrosion resistance caused by Ag. Thereafter, alloying with Y had attracted much researches because Y shows relatively higher solubility in Mg matrix (the solute limit of Y in Mg is ~12.8% at 552 °C) and strong precipitation strengthening potentiality. Similar to Mg-Gd alloy, precipitation hardening promotes the development of Mg-Y series alloys. The precipitation sequence of Mg-Y alloy is quite the same to that in the Mg-Gd alloys.

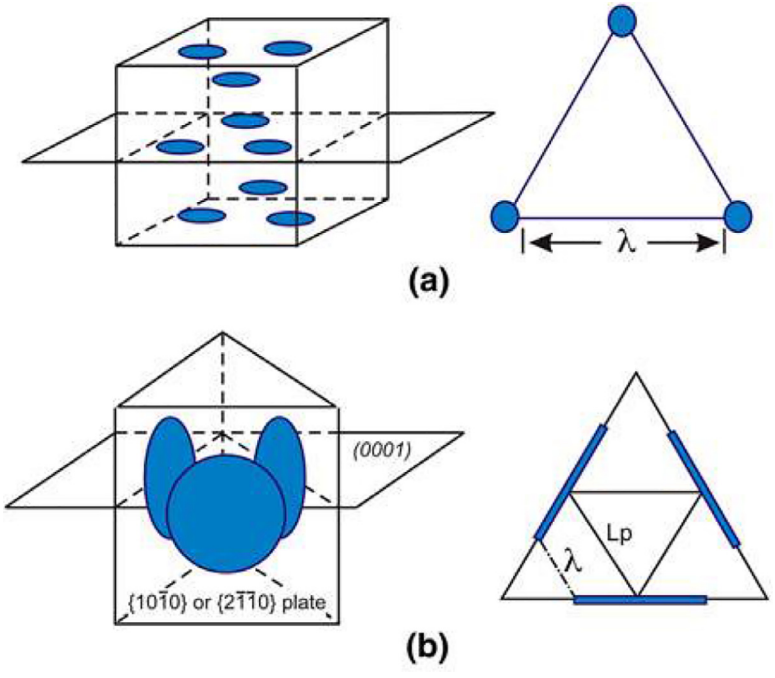

Fig. 3. Schematic diagrams showing (a) basal plane precipitates and (b) prismatic plane precipitates in Mg-RE alloys [24].

Table 1
Reported mechanical properties of Mg-Gd based alloys.

Series	Composition (wt.%)	Condition	Tensile properties			Heat treatment parameters	Ref.
			UTS (MPa)	YS (MPa)	E_f (%)		
Mg-Gd-Y	Mg-6Gd-3Y-0.4Zr	PM-T6	331	198	7.8	500°C × 8 h + 200°C × 80 h	[5]
	Mg-8Gd-3Y-0.4Zr	PM-T6	362	222	7.6	500°C × 8 h + 200°C × 80 h	[5]
	Mg-10Gd-2Y-0.4Zr	PM-T6	362	239	4.7	490°C × 8 h + 225°C × 16 h	[5]
	Mg-10Gd-3Y-0.4Zr	PM-T6	370	241	4.1	500°C × 8 h + 225°C × 16 h	[5]
	Mg-12Gd-3Y-0.4Zr	PM-T6	328	246	1.1	500°C × 8 h + 225°C × 16 h	[5]
	Mg-10.4Gd-3.3Y-0.46Zr	PM-T6	348	237	3	500°C × 6 h + 225°C × 16 h	[6]
	Mg-10Gd-1Y-Zr	PM-T6	215	135	12	525°C × 10 h + 250°C × 12 h	[7]
	Mg-10Gd-3Y-Zr	PM-T6	235	152	6.5	525°C × 10 h + 250°C × 12 h	[7]
	Mg-10Gd-5Y-Zr	PM-T6	300	285	~1	525°C × 10 h + 250°C × 12 h	[7]
	Mg-10Gd-3.74Y-0.25Zr	PM-T6	325	268	5.1	525°C × 6 h + 225°C × 24 h	[8]
	Mg-10Gd-3.74Y-0.25Zr	LF-T6	285	265	4.1	525°C × 6 h + 225°C × 24 h	[8]
	Mg-10Gd-3.3Y-0.41Zr	SQC-T6	383	264	1.5	480°C × 8 h + 225°C × 16 h	[9]
	Mg-6Gd-3Y-0.5Zr	*v*HPDC	248	173	17.5	as-cast	[27]
	Mg-10Gd-3Y-0.8Al	PM-T6	353	227	3.5	520°C × 6 h+550°C × 7 h+200°C × 48 h	[10]
	Mg-10Gd-3Y-0.8Al	PM-T6	301	213	12.1	520°C × 6 h+550°C × 7 h+225°C × 32 h	[10]
Mg-Gd-Sm	Mg-6Gd-2Sm-Zr	PM-T6	230	108	19.8	500°C × 4 h + 225°C × 32 h	[12]
	Mg-8Gd-2Sm-Zr	PM-T6	329	195	7.7	500°C × 5 h + 225°C × 8 h	[12]
	Mg-10Gd-2Sm-Zr	PM-T6	347	237	3.2	500°C × 6 h + 225°C × 4 h	[12]
Mg-Gd-Nd	Mg-6Gd-2Nd-Zr	PM-T6	342	182	7.9	500°C × 6 h + 200°C × 24 h	[13]
	Mg-8Gd-2Nd-Zr	PM-T6	342	200	5	515°C × 4 h + 225°C × 12 h	[13]
	Mg-11Gd-2Nd-Zr	PM-T6	353	224	3.7	525°C × 4 h + 250°C × 2 h	[13]
Mg-Gd-(RE)-Zn	Mg-10Gd-3Y-1.2Zn-0.4Zr	PM-T6	330	230	3	525°C × 72 h + 225°C × 16 h	[14]
	Mg-10Gd-3Y-1.0Zn-0.4Zr	PM-T6	364	253	2	500°C × 10 h + 225°C × 16 h	[6]
	Mg-17.4Gd-1.1Zn-0.6Zr	PM-T6	405	278	2.5	500°C × 12 h + 225°C × 8 h	[15]
	Mg-14Gd-3Y-1.8Zn-0.5Zr	PM-T6	366	230	2.8	520°C × 10 h + 225°C × 16 h	[16]
	Mg-6.5Gd-2.5Dy-1.8Zn	PM-T6	392	295	6.1	510°C × 10 h + 215°C × 109 h	[17]
	Mg-2.5Gd-1.0Zn-0.16Zr (at.%)	SCC-T6	366	260	3.3	500°C × 10 h + 200°C × 128 h	[18]
	Mg-14Gd-2Zn-0.5Zr	PM-T6	404	292	5.3	520°C 12 h + 200°C /64 h	[19]
	Mg-15Gd-1Zn-0.4Zr	PM-T6	405	288	2.9	500°C × 2 h + 520°C × 12 h + 200°C × 65 h	[20]
Mg-Gd-(RE)-Ag	Mg-18.2Gd-1.9Ag-0.3Zr	PM-T6	414	293	2.2	490°C × 10 h + 200°C × 36 h	[21]
	Mg-8.5Gd-2.3Y-1.8Ag-0.4Zr	PM-T6	403	268	4.9	500°C × 10 h + 200°C × 32 h	[22]
	Mg-15.6Gd-1.8Ag-0.4Zr	PM-T6	423	328	2.6	480°C × 18 h + 500°C × 8 h + 200°C × 32 h	[23]

* PM: permanent mold gravity cast, LF: lost foam cast, SQC: squeeze cast, *v*HPDC: vacuum high pressure die cast, SCC: semi-continuous cast.

Table 2
Reported mechanical properties of Mg-Y based alloys.

Series	Composition	Condition	Tensile properties			Heat treatment parameters	Ref.
			UTS (MPa)	YS (MPa)	E_f (%)		
Mg-Y-RE	Mg-3.5Y-2Nd-1.3Gd-0.4Zr	PM-T6	345	196	~7	525°C × 8 h + 200°C × 96 h	[29]
	Mg-4Y-4Sm-0.5Zr	PM-T6	348	217	6.9	525°C × 8 h + 200°C × 16 h	[30]
	Mg-10Y-2.5Sm	PM-T6	216	–	3.5	540°C × 6 h + 250°C × 2 h	[31]
	Mg-3.4Y-1.9Nd-0.9Gd-0.4Zr	SGC-T6	312	202	6.2	525°C × 8 h + 200°C × 136 h	[32]
	Mg–3.0Y–2.5Nd–1.0Gd–0.5Zn–0.5Zr	PM-T6	324	186	9.7		[33]
	Mg–3.0Y–2.5Nd–1.0Gd–0.5Zn–0.5Zr	SGC-T6	320	192	7.2		[33]
Mg-Y-(RE)-Zn	Mg-4.3Y-3Nd-1.2Gd-0.2Zn-0.5Zr	SGC-T6	316	214	4.4	525°C × 6 h + 225°C × 40 h	[34]
	Mg-4Y-2.4Nd-0.2Zn-0.4Zr	PM-T6	330	265	6.5	500°C × 6 h + 225°C × 16 h	[35]
	Mg-4Y-2.4Nd-0.2Zn-0.4Zr	PM-T6	339	268	4.0	500°C × 6 h + 200°C × 64 h	[35]
	Mg-11Y-5Gd-2Zn-0.5Zr	PM-T6	307	240	1.4	535°C × 20 h + 225°C × 24 h	[38]

*SGC: Sand mold gravity casting.

The Mg-Y-Nd ternary alloy has long been studied due to its combined precipitation strengthening and good ductility. Two commercial series Mg-RE alloys, WE43 and WE54 alloys, were developed which possessed good properties up to 250 °C and 300 °C respectively. The WE43 alloy retains its properties at high temperature far in excess of 5000 h, whereas WE54 retains its properties at high temperatures for up to 1000 h [28]. Other Mg-Y-*X* (*X* stands for Sm, Gd, Zn, etc.) alloys [29-35] were also reported to exhibit high strength (as shown in Table 2). For instance, the Mg-4Y-4Sm-0.5Zr alloy [30] can obtain comparable yield strength to that of WE43 alloy with nearly the same REs content.

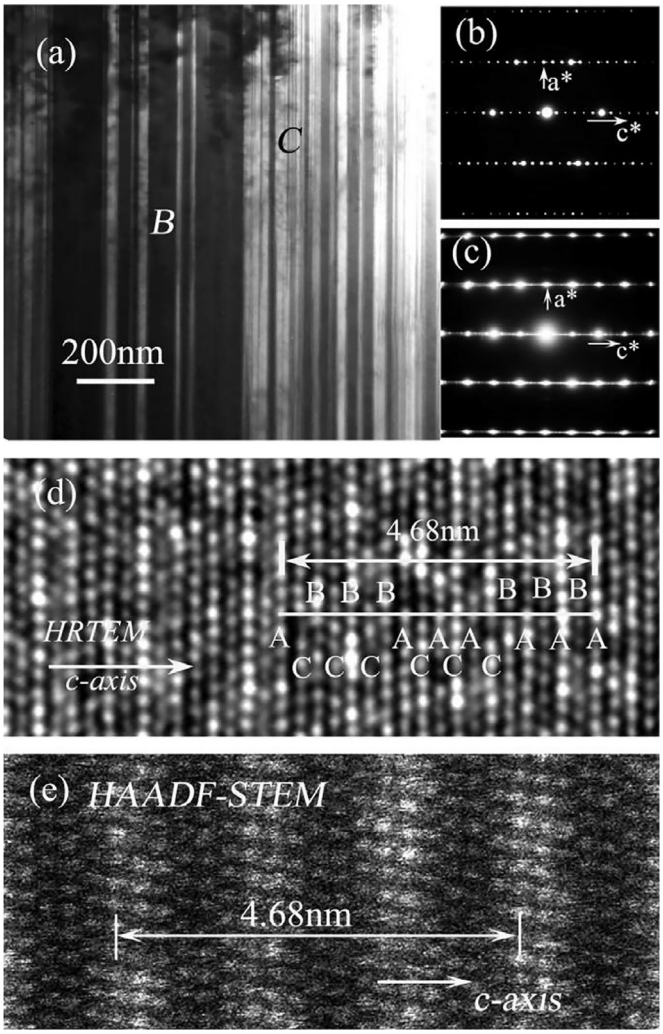

Fig. 4. TEM bright field micrographs at (a) the grain boundary of as-cast Mg-1Zn-2Y (at.%) alloy, and selected area diffraction patterns along $\langle 11\bar{2}0\rangle$Mg direction showing (b) the 18-R structured LPSO phase and (c) 2H-Mg with lots of stacking faults. (d and e) HRTEM and HAADF STEM images, respectively, revealing the stacking ordered as well as chemically ordered LPSO structure [37].

As indicated in Section 2.1, the LPSO phase can be formed in Mg-RE alloys by alloying with Zn, Cu, Co or Ni [36], and was mainly segregated at grain boundaries (typical TEM structure of LPSO phase as shown in Fig. 4 [37]). The developed microstructure provides scientists insights that LPSO-containing Mg-RE alloy might be a new candidate for creep resistant Mg alloy. Therefore, the Mg-11Y-5Gd-2Zn-0.5Zr alloy [38] was developed. The solute REs contents actually exceed the real solubility limits, and the insoluble REs reacts with Zn forming the LPSO phase to strengthen the grain boundaries.

3. Castability, purification and grain refinement of MG-RE alloys

During melting process of Mg alloys, many key factors should be considered such as castability, molten metal reactivity and grain structure control. This section will describe these three aspects of Mg-RE alloys. Other issues related to melting process was not introduced here due to limited space.

3.1. Castability

According to Mordike [39], castability of Mg-RE-(Zn)-Zr alloys containing elements such as Zn, RE, Ag and Y do not present any problems, which is because of the extremely efficient grain refining effect of Zr combined with relatively high volume fractions of eutectic phase. At present, the reports on castability of Mg-RE alloys are relatively few due to their good castabilities. However, for the castings with large-size and complex structure made from Mg-RE alloys, the mold filling characteristics should be taken into account. The spiral mold filling test is capable of ranking different alloys in a relative way, the typical casting is shown in Fig. 5(a) and (b) [40]. Li et al. [40] investigated the effect of pouring temperature, mold preheating temperature and flame-retardant content in molding sand on the fluidity of sand-casting Mg-10Gd-3Y-Zr alloy. The increase of pouring temperature leads to decrease of fluidity if the pouring temperature is higher than 750 °C (as shown in Fig. 6(a)). The use of flame retardant in molding sand can generally lead to enhancement of fluidity of the Mg-RE alloy. The increases of mold pre-heating temperature lead to improvements in fluidity (as shown in Fig. 6(b)) while also leads to coarsening of grains. The use of reclaimed sand was also studied as a route to achieve effectively economic and environmentally friendly use of raw materials in engineering practice. Li et al. [41] found that addition of 0∼20% reclaimed sand to the new sand showed limited detrimental effect to the molding sand when considering the strengths and residual stress. Huang et al. [42] showed that the fluidity of Mg-Nd-Zn-Zr alloy cast by permanent mold depended on the pouring temperature and mold temperature. A better fluidity could be obtained when pouring and mold temperatures were within 760∼790 °C and above 350 °C for NZ30K alloy, respectively.

Huang [43] investigated the effect of flux refining, pouring temperature and mold types on the fluidity of Mg-10Gd-3Y-Zr Mg alloy. It was shown that spiral length could be increased from 780 mm to 1270 mm by flux refining, or from 595 mm to 995 mm by increasing pouring temperature from 690 °C to 770 °C, respectively. The mold made from tectorial sand was found to improve the fluidity than iron mold. These findings are very useful for industrial engineers since the Mg-Gd-Y alloy is normally used as low pressure sand cast components (please find details in Section 4.1.1).

Another very important factor belonged to castability such as hot tearing susceptibility (HTS) of Mg-RE alloy can be referred to a recent review work by Song et al. [44]. Huang [43] investigated the HTS of Mg-10Gd-3Y-Zr alloy with constrained rod method (as shown in Fig. 5(c) and (d)). Mg-10Gd-3Y-Zr alloy was found to have a much lower HTS (value 8) than that of AZ91D alloy (value 32).

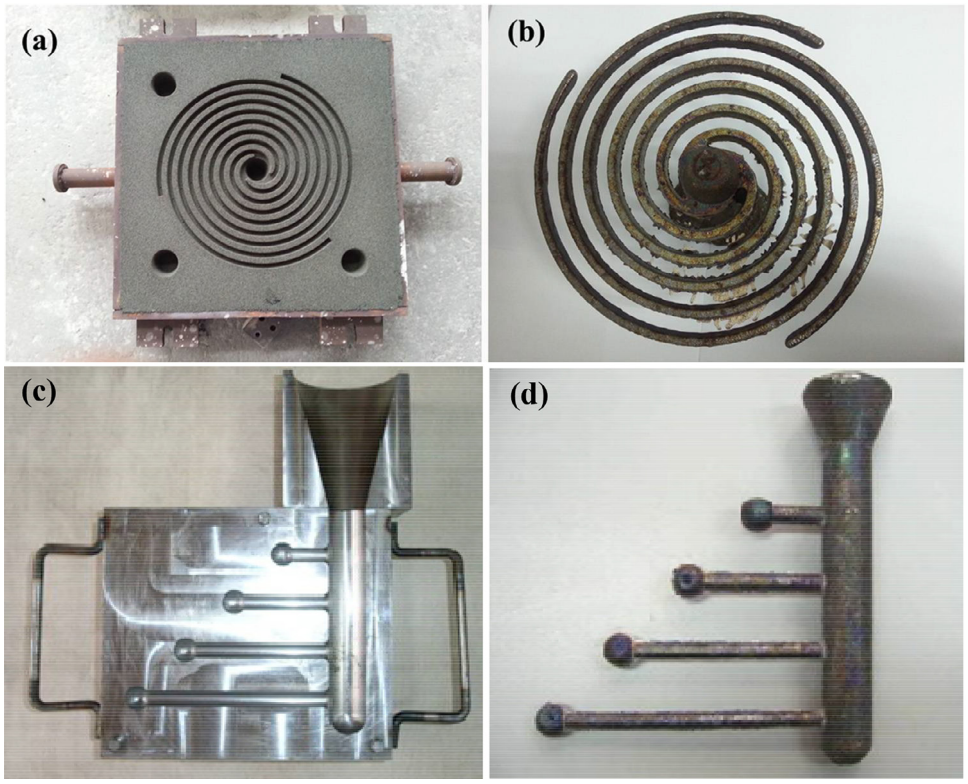

Fig. 5. Photograph of (a) three spirals mold used to evaluate fluidity and (b) typical casting [40]; and (c) hot crack rod mold and (d) typical casting [43].

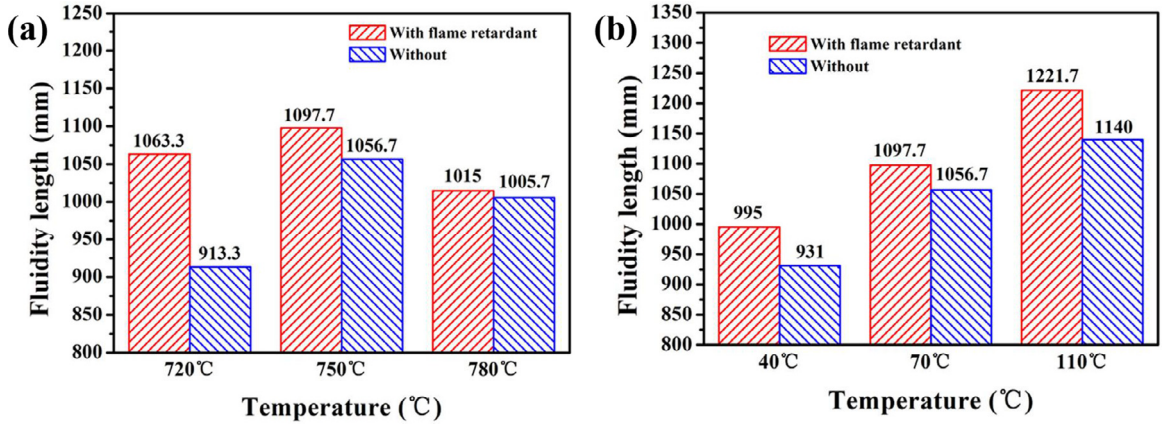

Fig. 6. The influence of (a) pouring temperature and (b) mold pre-heating temperature together with or without the use of flame retardant in molding material on fluidity of sand cast GW103K alloy. [40].

3.2. Melt purification of MG-RE alloys

3.2.1. Importance of purification

During melting process, the high activity of Mg makes the alloy melt easily burned by absorbing O_2 or moisture and contaminated by forming inclusions, which implies that the ignition proof work and purification work is greatly necessary. The burning can be prevented by special flux and protective gas such as $SF_6 + CO_2$. However, the inclusions are hard to avoid, and should be removed by various purification methods.

Nonmetallic inclusions are easily produced during melting of Mg alloy, among which MgO inclusion is the most common one. Non-metallic inclusions decrease the metal fluidity, which could result in poorer castability by changing the solidification parameters [39]. Fig. 7 shows the example of typical nonmetallic inclusions in Mg-10Gd-3Y-0.5Zr (GW103K) Mg-RE alloy. The inclusions exhibit spherical, bar-shape and irregular morphologies, which are believed to be harmful. The inclusions cut off the continuity of the matrix, cause stress constrain, supply flaw recourses and thus damage the mechanical properties and corrosion resistance seriously [45].

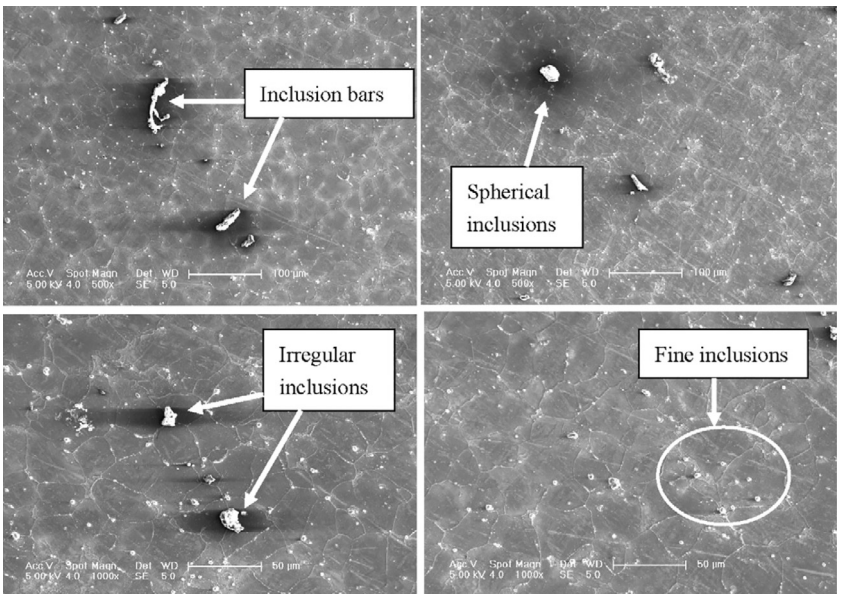

Fig. 7. Morphology and distribution of nonmetallic inclusions in GW103K alloy [45].

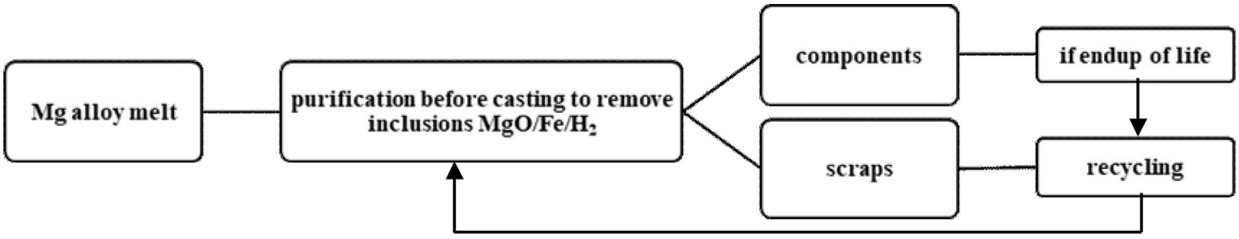

Fig. 8. The route for Mg alloy purification.

Metallic inclusions, such as Fe, Ni and Cu, as impurity element, can be introduced not only from the raw materials but also from the use of Fe crucible (especially after the coating on crucible being destroyed at high temperature). Even with a small amount, impurity elements especially Fe can severely deteriorate the corrosion resistance of magnesium alloys [46]. Moreover, H_2 gas can be absorbed into Mg alloy when the heating of flux is not enough or the environment is wet during melting. Gas induced porosities are a serious defect of Mg alloys, because the local solidification rate is lower in such gas regions, leading to shrinkage porosity [47]. From these analyses, it can be seen that melt purification is very important during melting of Mg-RE alloys.

In addition, in die-casting operations of Mg alloy, around 50% of the melt is converted into scraps which contain biscuits, sprues, runners, flash, overflows, dross, sludge, scrap parts and so on. These scraps can be recycled for re-use when suitable purification technology is adopted. Fig. 8 plots the route for Mg alloy purification.

3.2.2. Methods of purification

During the past decades, various purification methods have been developed, such as flux purification, non-flux purification and complex purification methods [48].

(i) Flux purification. Flux purification is a very old but effective method. In this process, nonmetallic inclusions can be wetted, absorbed by the special flux containing $MgCl_2$, and then form $MgCl_2$•5MgO compounds sinking to the bottom of crucible [49]. However, rare earth elements, such as Gd and Y, can react with $MgCl_2$, which results in the loss of RE. Therefore, special refining agents with the addition of $GdCl_3$ [45] or YCl_3 [50] have been developed to suppress/compensate the loss of Gd or Y. The “suppression mechanism” could be ascribed to the decline in Gibbs free energy which slows down the rate of reaction between $MgCl_2$ and Gd [45] or Y [50].

(ii) Non-flux purification. It includes filtration purification, gas bubbling purification and so on, in which the flux is not used. The most effective one is to use filter as shown in Fig. 9 [50]. Due to the complex net inside, the filter absorbs or captures the inclusions very effectively. Among the filters, ceramic foam filter (CFF) has been widely used because it is easily operated (Fig. 9).

Gas bubbling is a new method with a much higher ability to degas and remove inclusion, as shown in Fig. 10 [51]. The purification mechanism can be explained by Fig. 11: the inclusion approaches the gas bubble (Fig. 11(a)); collision occurs, and a thin liquid melt film builds up (Fig. 11(b)); inclusion oscillation and sliding on the surface of the bubble (Fig. 11(c)); inclusions attach to the bubble surface, then float up or slide

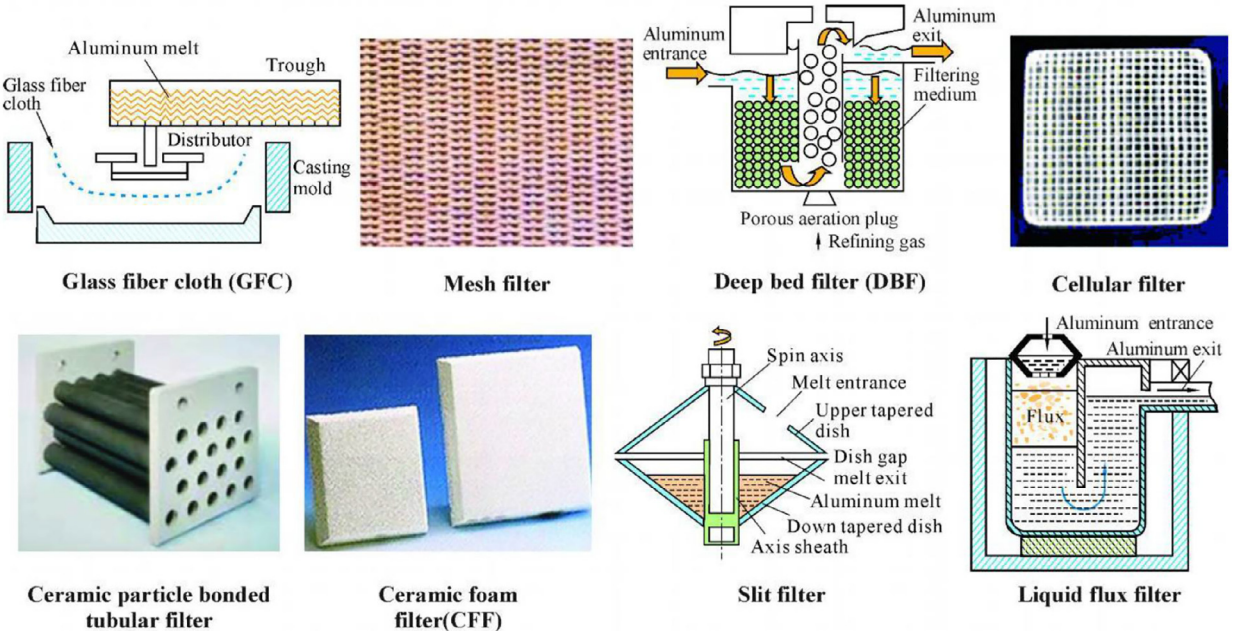

Fig. 9. Various kind of filters used in casting process of Al melt [50]. Among them, CFF has already been used in Mg melt, and it is also expected that other filters could be used in Mg melt.

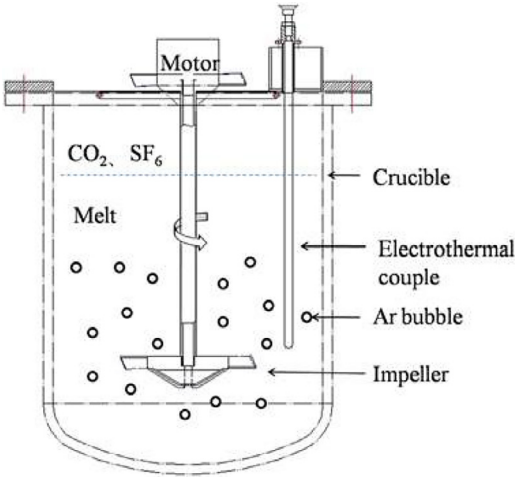

Fig. 10. Schematic drawing of rotating impeller gas bubbling system [51].

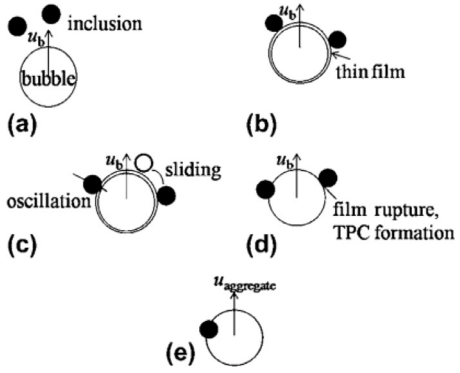

Fig. 11. Process of inclusion removal by gas bubble floatation (u_b bubble floating velocity; $u_{aggregate}$ aggregation floating velocity; and TPC three-phase contact). The detailed explanations for each sub-figure can be found in the above texts [51].

away and detach (Figs. 11(d) and (e)). Mei et al. [51] investigated the effects of rotating gas bubble stirring process parameters (Ar flow rate, time, and rotating speed) on purifying effectiveness of sand-cast Mg-10Gd-3Y-0.5Zr alloy. The results show that too high or too low Ar flow rate is unfavorable for inclusion-removal, and a high rotary speed of spraying gas is helpful to improve the inclusion-removal efficiency.

(iii) Complex purification. This method is not new because it just combines different kinds of purification method together, and is reported to be more efficient than traditional single method. For example, flux purification method can be combined with gas bubbling or filtration purification. Mei et al. [52] reported that the new complex refining method (flux plus rotating gas bubble stirring) can significantly decrease the volume fraction of inclusions from 0.47% to 0.28%, which then improves the mechanical properties.

At present, the work on purification of Mg-RE alloy is relatively less than that of Mg-Al alloy, which is partly because that RE itself has certain ignition-proof effect and purification effect. This helps reduce the inclusion amount during melting. However, new purification methods still need to be developed aiming at the application in large-scale melting of Mg-RE alloy in industry production.

3.3. Grain refinement of MG-RE alloys

3.3.1. Addition of ZR

The HCP crystal structure of Mg results in poor ductility and formability at room temperature. Thus, the grain refinement work is very important. For Mg-RE alloys, the most

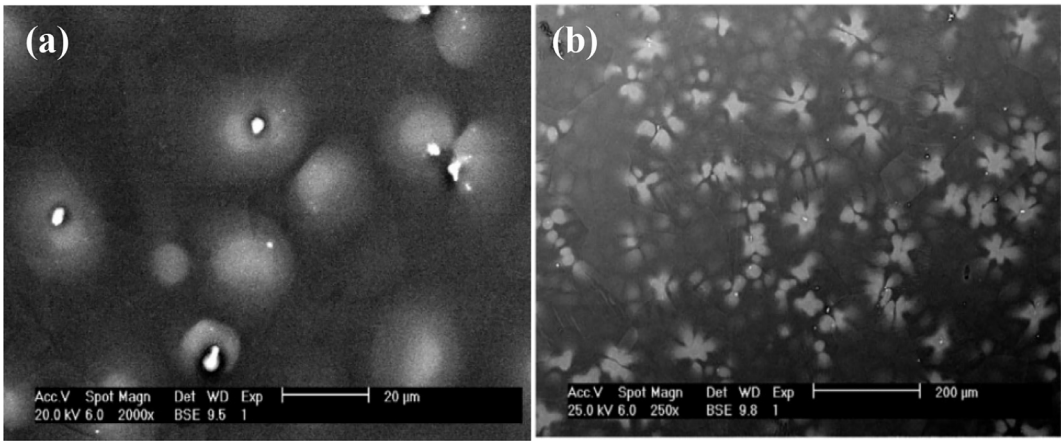

Fig. 12. Growth morphologies of Zr-rich halos in: (a) Mg-0.55Zr, and (b) Mg-0.32Zr alloys [57].

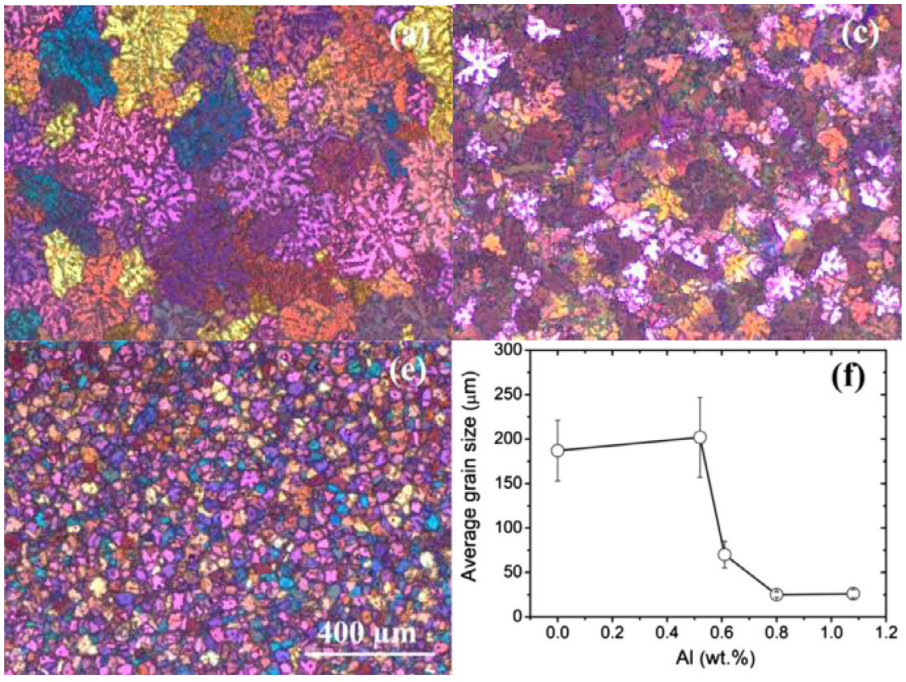

Fig. 13. Optical microstructure of Mg-10Gd-3Y alloy refined by various Al contents: (a) 0%, (c) 0.62%, (e) 1.08%, and (f) variation in grain size [67].

effective grain refiner is Zr [53,54], which was discovered in 1930s. This is totally different from the grain refinement of Mg-Al alloys, because Al can react with Zr removing the grain refinement effect of Zr. At present, Zr is normally added through the Mg-Zr master alloy to avoid the difference of melting point between Zr (1852 °C) and Mg (650°C). The mechanisms of grain refinement by Zr have been well understood. Zr has the same *HCP* crystal structures with Mg, and the small lattice disregistry between Zr ($a = 0.323$ nm, $c = 0.514$ nm) and Mg ($a = 0.320$ nm, $c = 0.520$ nm) makes Zr an ideal heterogeneous nucleating substrate for Mg [53,55]. The peritectic reaction at 654 °C for a saturated Zr content of 0.58% [55] plays an important role in grain refinement, which shows that zirconium-rich phase precipitates from the liquid and reacts with magnesium to form an magnesium phase [55,56]. This peritectic reaction can be well justified by the Zr-rich haloes observed in the microstructure as shown in Fig. 12 [57]. However, recent study has shown that, even at a much lower Zr content (far below the peritectic point), significant grain refinement effects can also be achieved. This can be explained by the strong constitutional supercooling effect (i.e. growth restriction factor, GRF). The soluble Zr generates a very high GRF value (38.29) compared with most of other elements (normally around 1∼6) in Mg [53].

Grain refining effect of Zr on Mg-RE alloy can be influenced by the cooling conditions due to the interactions among thermal supercooling, constitutional supercooling and nucleation events. Pang et al. [58] found that, as the cooling rate increased from 0.7 °C to 3.6 °C, the grain size of sand mold cast Mg-10Gd-3Y-0.5Zr alloy was decreased from 59 μm to 39 μm, and the hardness and tensile strengths were increased continuously. Pang et al. [59] also found that

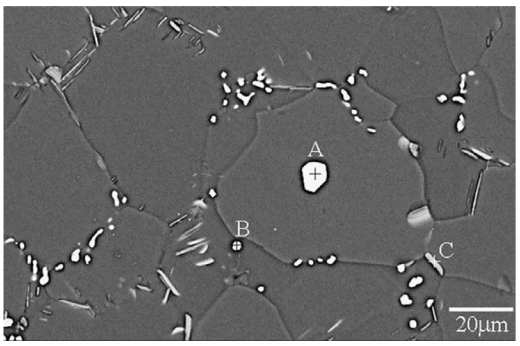

Fig. 14. Typical SEM microstructure of Mg-10Y-1Al alloy showing the grain refining substrate Al_2Y phase (particle A) [66].

the increase of pouring temperature from 680 °C to 750 °C in sand mold casting lead to the increase in nucleation undercooling of α-Mg phase from 2.3 to 6.3 °C through the computer aided cooling curve analysis [60,61], which eventually increased the grain size from 44 μm to 71 μm. Nevertheless, grain coarsening was recently found to occur in Mg-Y alloy refined by Zr at cooling rate above 160 K/s [62]. Explained by the Interdependence model, the size of the constitutionally supercooled zone was reduced by the higher thermal gradient and this effect promoted the continued growth of grains rather than further nucleation events.

The most serious problem during Zr alloying is the settling of Zr particles. Because the density of Zr (7.8 g/cm^3) is much higher than Mg (1.7 g/cm^3), Zr particles quickly settles down to the bottom of crucible during melting of Mg alloy according to Strokes' law, which finally causes the loss of expensive Zr element and even grain coarsening [63]. Therefore, the development of a better Mg-Zr master alloy is necessary, and when the particle size distribution is confined to be within 1∼5 μm, the utilization rate and grain refinement effect of Zr is more satisfactory [64]. In addition, in order to avoid the settling of large Zr particles, other method for alloying with Zr has also been tried, such as K_2ZrF_6-KCl-NaCl salts mixture [65]. The mixture also showed good refinement effect. However, the inclusions remaining in the melt are difficult to remove. If the salt route is used, an efficient purification flux should be developed.

3.3.2. Addition of Al

Recently, Al has been reported to be a promising grain refiner for Mg-RE alloy. A small addition (∼1%) of Al is enough for significant grain refinement effect on Mg-RE alloy. The mechanism for grain refinement is attributed to the formation of active nucleating Al_2RE particles, such as Al_2Y [66], Al_2Gd [67], Al_2Sm [68], and Al_2Ce [69]. Fig. 13 is an example showing the effect of Al content on grain refinement of Mg-10Gd-3Y alloy, which shows the grain size can be refined from ∼200 to ∼20 μm [67]. Fig. 14 shows the morphology of active nucleating Al_2Y particles [66]. The optimum size of active Al_2Y nucleation particles corresponding to the most effective grain refinement for Mg-10 wt.% Y cast alloy is 6∼6.5 μm. In general, Al_2Y particles that are smaller than 2 μm do not act as heterogeneous nucleation sites. Moreover, cooling rate was reported to influence the size and number density of Al_2Y particles, which finally influenced the grain refinement efficiency [67]. This means that for castings with large sizes in factory, the efficiency of grain refinement by Al should be carefully investigated since the cooling rate may vary between each position.

4. Materials fabrication or processing of MG-RE alloys

4.1. Precision liquid processing for MG-RE alloys

With an aim to eliminate or reduce the additional energy or material costs in cutting and surface machining of casting components, the pursue of net shape forming or near net shape forming has raised the rapid development of precision liquid processing techniques. Conventionally, Mg-RE alloy castings are fabricated by steel mold (permanent mold) or sand mold based gravity casting. The uprising development of precision liquid processing of Al and Mg-Al series alloys also draw attentions to the Mg-RE alloys regime, which includes low pressure sand cast (LPSC), high pressure die cast (HPDC) and squeeze cast (SQC), etc.

4.1.1. Low pressure sand cast

The need for clean Mg alloy melt (without casting defect) as well as complex structures are increasingly important in engineering practice. Low pressure sand casting (LPSC) technology are meeting these requirements while with a loss of productivity. The Mg alloy melts are prone to oxidation, and as mentioned in Section 3.1, the purification of Mg alloy melt is tougher than Al alloy melt due to the inclusions being always denser than the environmental melts. Hence, the effects in preventing melt contamination is essential in the fabrication process. Low pressure sand casting utilizes the applied gas pressure to push the alloy melt to flow antigravity into the gating system of the mold through a submerged ceramic pipe at the middle of the alloy melt tank (as shown in Fig. 15(a) [70]). The quality of the Mg-RE alloy melt is thus promised by the process. Furthermore, the casting components with large size and thin-walled complex structures can be fabricated through LPSC process due to the flexibility of sand mold core and cavity. The Mg-RE castings with maximum length of 1700 mm and minimum thickness of 2∼5 mm were successfully fabricated by LPSC (as shown in Fig. 15(b) [70]. The success in fabricating thin-walled casting components are proofs that the antigravity melt flow and exerted pressure during solidification are beneficial to obtain sound surface quality, high dimension accuracy and less of shrinkage microporosity. The study on LPSC Mg-6Gd-3Y-0.5Zr alloy by Zhou et al. [71] through the Niyama criterion found that exerting of holding pressure can effectively reduce the amount of shrinkage microporosity. Therefore, the mechanical strengths, including the quasi-static tensile strength and high cycle fatigue strength of LPSC Mg-RE alloys were improved when compared with conventional

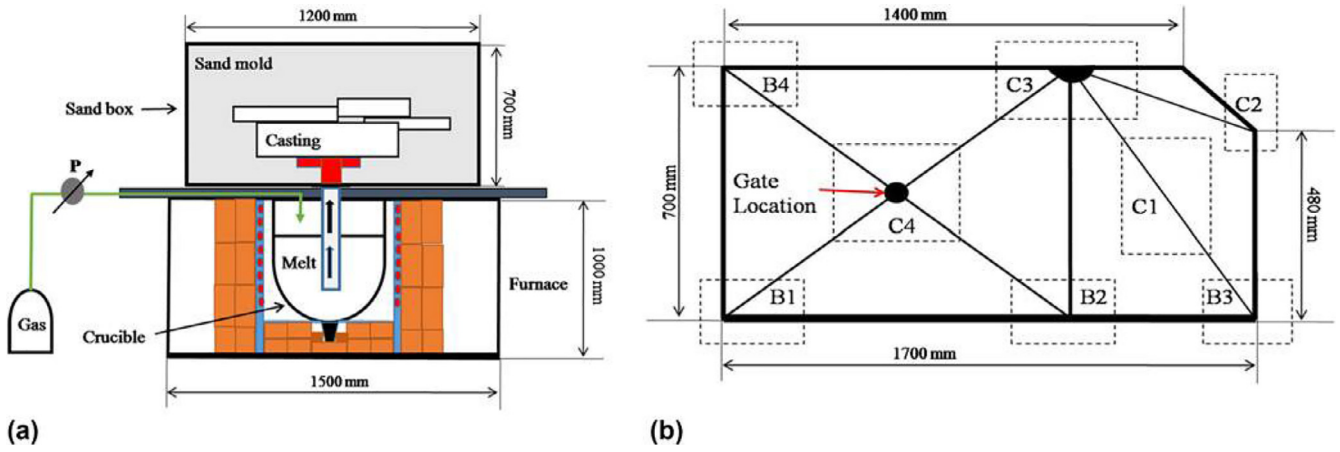

Fig. 15. Schematics of (a) the low pressure sand cast facility and (b) the simplified illustration of Mg-RE alloy casting with large size and thin-walled complex structures [70].

gravity casting, and the application of LPSC in aerospace area has been the main application of Mg-RE alloy.

In the LPSC process, the processing parameters, for instance, pouring temperatures, cooling conditions, holding pressure, mold pre-heating temperature and the sand mold materials, etc., are crucial factors. These factors can influence the solidification behavior, the as-cast microstructures and following heat treatment procedures and mechanical properties of the final castings. There is no doubt that such casting parameters are really important in engineering practice, while systematic study on the parameters is not available from published works. A similar study by Fu et al. [72] on low pressure die cast AM60 alloy can partly show how these parameters may affect the casting process.

Due to the relatively low cooling rates during solidification, the heat treatment procedures of LPSC Mg-RE alloys are quite varied with conventional permanent steel mold cast. The T6 heat treatment parameter of LPSC GW103K alloy is solution heat treatment at 525 °C for 6 h followed by aging treatment at 250 °C for 10 h, while it is 500 °C × 6 h and followed by 225 °C × 16 h for permanent steel mold cast counterpart [73,74]. The consequent coarser grains in LPSC Mg-Gd-Y alloy lead to a slight decrease of room temperature YS, while a significant improvement of UTS and E_f. The elevated temperature strengths [75] and high cycle fatigue strengths [76] were also improved in LPSC castings. Other trials in LPSC Mg-3Nd-0.2Zn-0.4Zr [77] and Mg-4Y-2Nd-1Gd-0.4Zr [78,79] alloys also confirmed similar conclusions by the analysis of heat treatment procedures, tensile and fatigue properties.

4.1.2. High pressure die cast

HPDC is a kind of near-net shape forming technique, which utilize a relatively small amount of alloy melt and leave nearly no space for further cutting processing. The advantages of HPDC technique include: (1) the relatively higher productivity of the operation procedures, (2) the relatively higher cooling rates allowing finer microstructure and better mechanical performance, (3) good surface quality, shape and dimension accuracy, and (4) highly automated machine and environmental friendly.

Mg alloy melt shows a relatively good fluidity at temperatures with ~100 °C superheating. Hence, the castability of Mg alloys is promised [80]. The alternation from engineering plastics to thin-wall Mg castings has thus been developed in the 3C industries for decades, which moves forward to the rapid development of HPDC Mg parts or components. The HPDC Mg-Al and Mg-Al-RE alloys such as AZ91 and AE42 [81] have long been researched and much progresses were made towards engineering applications. For Mg-RE alloys, efforts have been made in Mg-Gd-Dy-Zr [82], Mg-La-RE (Nd, Y or Gd) [83] and Mg-Nd-Zn-Zr [84] alloys by conventional HPDC. However, the HPDC Mg-RE castings cannot be further strengthened by solution heat treatment, because the entrapped porosities during HPDC process may lead to surface blistering during subsequent heat treatments. Thus, the age-hardening effect cannot be exerted.

Recently, vacuum assisted HPDC has made it possible to allow HPDC Mg-RE alloy castings to undergo a moderate level of heat treatment due to the reduction of porosities. Fig. 16 [85] shows an example of vacuum assisted HPDC system designed by BCAST at Brunel Univ. Li et al. [27] showed that vacuum assisted HPDC Mg-6Gd-3Y-0.5Zr castings can be solution heat treated at 475 °C for 2 h [27], which allow a relatively huge quantity of age hardening potentiality. The room temperature YS, UTS and E_f of Mg-6Gd-3Y-0.5Zr alloy were greatly improved from 143 MPa, 196 MPa and 3.7% in conventional HPDC to 173 MPa, 248 MPa and 17.5% in vacuum HPDC counterparts, respectively. However, the vacuum assisted HPDC casting may not been widely promoted if considering the relatively high cost and low productivity when compared with conventional HPDC. The other reason for the slow development of HPDC Mg-RE alloys may lie in the external solidified crystals and the skinning effect cannot be eliminated. The external solidified crystals will cause unpredicted failure of casting at surface or inner area, and the skinning effect will lead to a segregation of REs at casting surfaces and harmful to the overall mechanical performances.

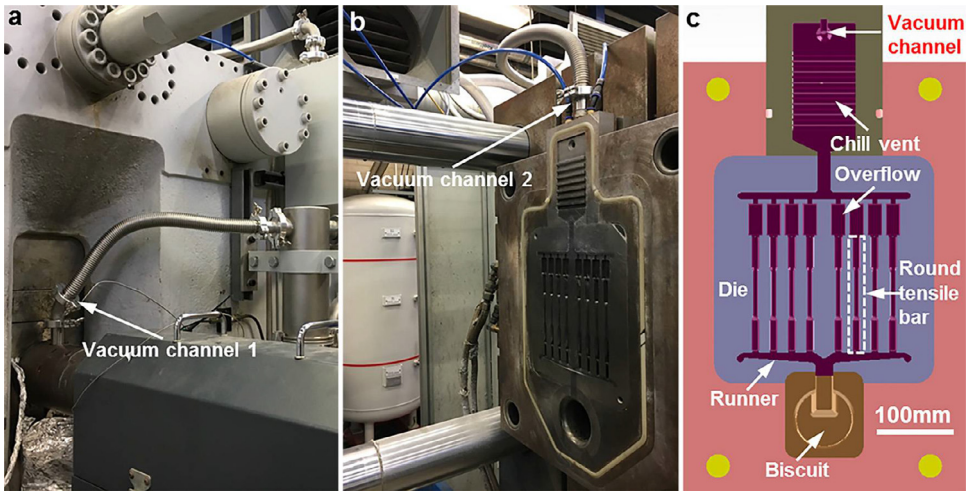

Fig. 16. The setup of two-stage super vacuum assisted HPDC system by BCAST [85], (a) one channel at shot sleeve and (b) one channel at the top of die cavity, and (c) the cross section of die-set showing the location of round tensile test samples designed according to ASTM B557.

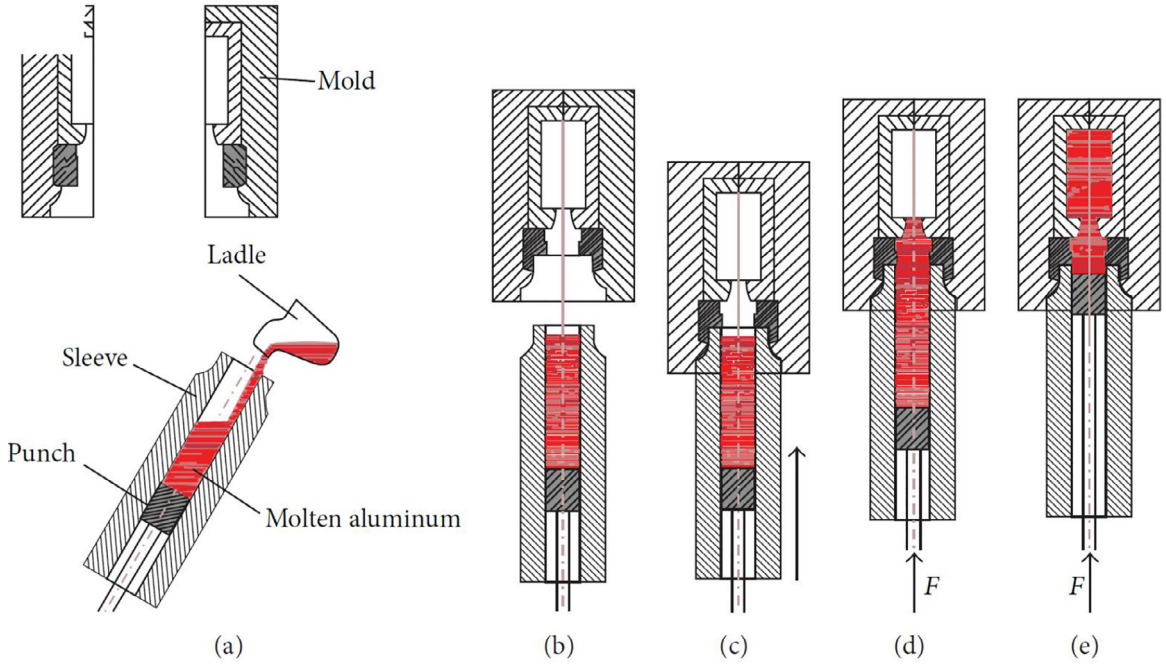

Fig. 17. Schematic illustration showing the indirect squeeze casting process: (a) molten alloy was poured into heated sleeve after the sleeve has tilted, (b)-(c) sleeve was moved back to its original position and rose to cooperate with mold, (d) punch rose fast until molten alloy got to flow gate, and (e) molten alloy was slowly filled to cavity and solidified under pressure [88].

4.1.3. Squeeze cast

Squeeze casting combines casting and forging into a single step by applying pressure during solidification of the alloys (Fig. 17). The superimposed pressure limits gas entrapment during die filling, thereby allowing for subsequent solution treatment of the alloys. Moreover, the application of an external pressure during solidification provides several advantages, including: (1) enhancing the cooling rate by increasing the heat transfer rate between the alloy melt and the mold wall; (2) eliminating casting porosity, shrinkage, and reducing the tendency for hot tearing during solidification; and (3) limiting the development of macroscopic solute segregation by restricting atomic movement [86,87].

Squeeze casting has been applied to a variety of Al alloys and Al based composites [89–93], and to the Mg-Al [94] or Mg-Zn [95] alloys systems. It is shown that some effects could be obtained, such as less porosity than HPDC castings, better heat treatment tolerant temperature range than HPDC and PMC (permanent mold casting), good surface quality as to fulfill the basic requirements for precision forming, and more importantly, better mechanical performance than conventional HPDC and PMC casting alloy.

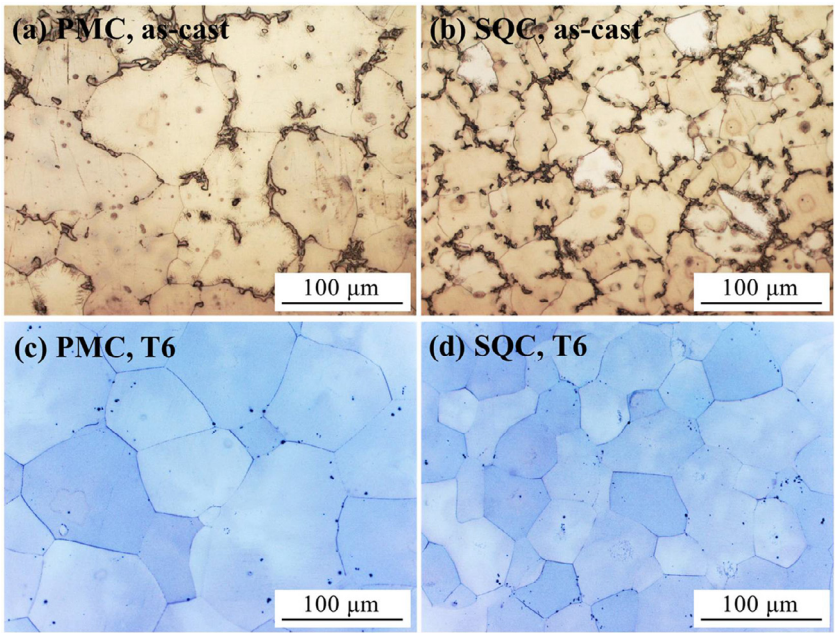

Fig. 18. Optical microstructures of (a), (b) as-cast and (c), (d) as T6 heat treated GW103K prepared by (a), (c) permanent mold gravity cast (PMC) and (b), (d) squeeze cast (SQC), respectively [9].

Not long ago, squeeze cast was found to cause effective grain refinement of binary Mg-Nd alloys [96]. Based on this, systematic research work on squeeze casting of Mg-RE alloy has been carried out by Wang et al. [9,97]. The processing parameters, including applied pressure and pouring temperature, are critical factors that influence the microstructure of as-cast Mg-RE alloys. The applied pressure can effectively refine the primary Mg phase in Mg-Gd-Y alloy through increasing the nucleation rate and decreasing of critical heterogeneous nucleation size. The optical microstructures of GW103K alloy fabricated by permanent mold gravity cast and squeeze cast in both as-cast and as-T6 heat-treated conditions were compared in Fig. 18. It can be seen that, the refinement of grains is effective in as-cast and sustained to as-T6 heat treated condition. Under optimal process parameters, the TYS, UTS and E_f of squeeze cast GW103K alloy are 151 MPa, 232 MPa and 3.0%, respectively in the as-cast state, and 264 MPa, 383 MPa and 1.5%, respectively in the as-T6 heat treated state, both of which represent significant improvements over those of the PMC counterparts. Recent studies on Mg-Gd-Zn series alloys [98] also concluded that squeeze cast is a promising technique to improve both the strength and ductility of Mg-RE alloys.

4.2. Semisolid processing of MG-RE alloys

Semisolid forming is a material processing technique that utilizes the relatively low deformation resistance or the relatively quasi-liquid fluid ability at temperatures between solid and liquidus line of metals, which is thus termed as thixo-forming and rheo-forming, respectively.

In an attempt to achieve enhanced nucleation and restricted growth of primary Mg phases, various physical treatment procedures were introduced into the Mg alloy melt during the primary solidification process (from above liquidus line to semisolid temperature ranges). The final products, or the so-called semisolid slurries, treated by aforementioned physical processing routes are fine and globular primary Mg particles equally distributed or entrapped within liquid phases.

4.2.1. Slurry preparation techniques

Mechanical stirring is powerful for metal alloy processing by providing a strong shearing force. Various mechanical stirring facilities have been widely introduced in semisolid slurry preparation of Mg and Al alloys, for instance the conventional agitating blade, the twin screw shearing stirrer, and the newly developed mechanical rotational barrel [99]. Besides, physical treatments, for instance electromagnetic stirring, direct or indirect ultrasonic vibration, gas bubbling, etc. have also been introduced to the fabrication of semisolid slurries for Mg and Al alloys. The non-contact features of ultrasonic or electromagnetic stirring specifically fits the physical or chemical performances of Mg alloy melt.

In Mg-RE alloys system, there are only very few research literatures available. Fang and Lu et al. [100–102] successfully fabricated the semisolid Mg-3RE-1Zn-1.4Y alloy slurry by direct ultrasonic vibration technique, and achieved good results showing relatively fine primary Mg phases. Wu and his group members have established a system of low frequency electro-magnetic stirring (LFEMS) facility for slurry preparation as shown in Fig. 19, and carried out researches on the Mg-Gd-Zn [103,104] and Mg-Nd-Zn [105] series Mg-RE alloys. They have systematically studied the effects of processing parameters including applied voltage, rotational frequency and cooling rate on the microstructure of semisolid slurry of the Mg-Gd-Zn alloy, and found that all the factors have remarkable influences on the

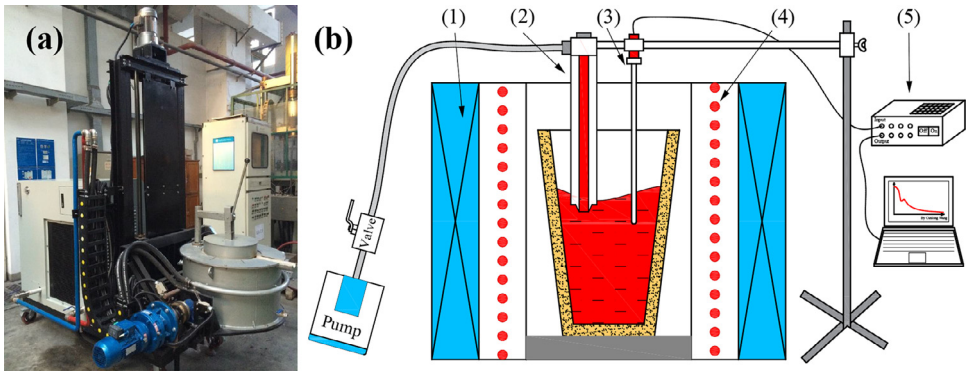

Fig. 19. The LFEMS semisolid slurry preparation facility (a) and a schematic illustration of the experimental apparatus (b). The numbers are stand for: (1) Magnetic coils, (2) Vacuum sample collection system, (3) Thermocouple, (4) Heating coils, and (5) Temperature recording system [104].

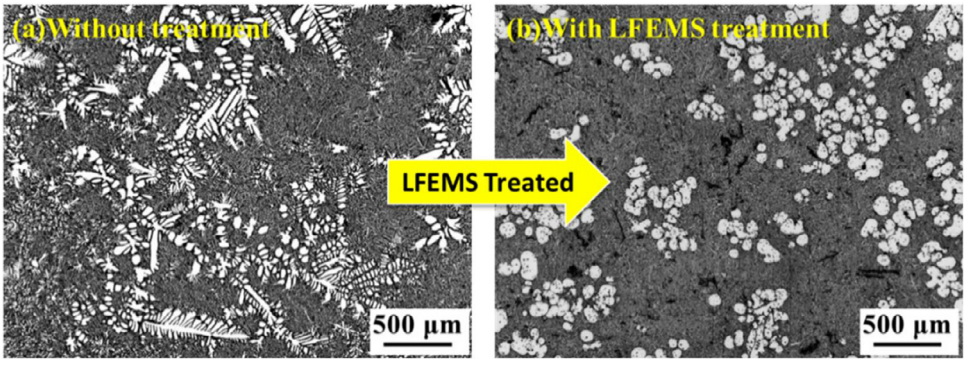

Fig. 20. Optical microstructures of semisolid Mg-Gd-Zn alloy slurries (a) before and (b) after low frequency electromagnetic stirring treatment for rheo-forming [103].

microstructures of the slurries. The LFEMS treatment leads to the evolution in morphology of primary Mg particles from dendritic to non-dendritic. Under the optimized parameters, fine and spherical primary Mg particles were obtained, and the average particle size of primary Mg phase was refined from ~680 to ~150 μm (as shown in Fig. 20). The dendrite fragmentation mechanism by which the semisolid Mg-RE alloys slurries were prepared was discussed, and the related criterion was also proposed [104]. Similar conclusions can also be obtained in the Mg-Nd-Zn alloys system [105].

A special semisolid slurry preparation method dedicated to the thixo-forming process is the iso-thermal hold technique. Wu et al. [106] have studied the influences of temperature and holding time on the formation of globular microstructure of Mg-Gd-Y-Zr alloy by isothermal holding treatment. The mechanism for the formation of non-dendritic microstructure in Mg-Gd-Y-Zr alloy is particle coalescence at 600 °C, while Ostwald ripening at 620 °C. Many semisolid slurry preparation techniques that have been previously proven effective in Al and Mg-Al alloys are currently introduced in the Mg-RE alloys. Obtaining fine and spherical semisolid slurries of Mg-RE alloys is the basis for both thixo-forming and rheo-forming of Mg-RE alloys.

4.2.2. Thixo-forming of MG-RE alloys

Thixo-forming of metals utilizes the conventional wrought (or cast) techniques to process the pre-heated billets within semisolid temperature ranges, where the billets were solidified through aforementioned slurry preparation methods. The processing force is thus severely decreased when compared with the force required for solid processing due to an increased processing temperature. The fine and globular primary particles of alloy can be "frozen" to room temperature, which can thus improve the mechanical performance of the alloy by grain boundary strengthening. Plenty of thixo-forming techniques have been invented, for instances the thixo-forging, thixo-extrusion [107], etc. In Mg-Al series alloys, thixo-extrusion has been proven to be a unique route to fabricate rods with excellent mechanical properties, while there is still limited report available on thixo-forming of Mg-RE alloys. The thixo-forming possibilities of Mg-10Gd-3Y-0.5Zr [106], Mg-8Gd-4.48Y-3.34Zn-0.36Zr [108] and Mg-5.15Y-3.75Gd-3.05Zn-0.75Zr [109] alloys were evaluated through the isothermal holding treatment technique. It was shown that homogenous spherical primary Mg phase could be obtained under optimal parameters of reheating temperature and isothermal holding time. However, the parameters were quite varied if the solute REs were different. Xie et al. [110] utilized as-cast and as-extruded Mg–8.20Gd–4.48Y–3.34Zn–0.36Zr alloy rods as raw billets and prepared the cup-shaped castings through the thixo-forming process (as shown in Fig. 21), and found that castings without macro-defects and micro-defects could be formed at forming temperature of 580 °C. The mechanical properties revealed

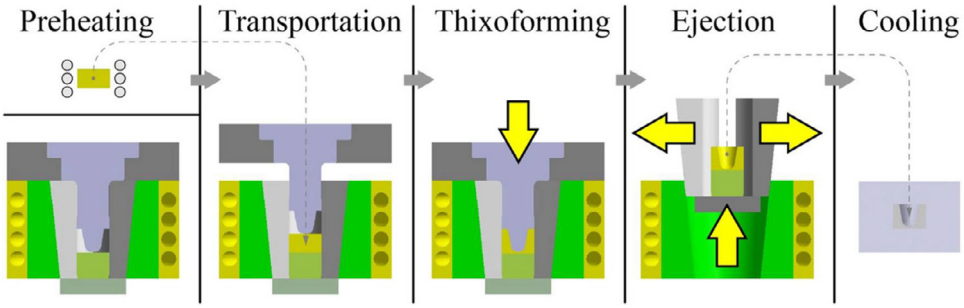

Fig. 21. Schematic diagram of thixo-forming strategy [110].

that the applied load could effectively influence the strength at the cup bottom area, while showed limited impacts on the wall area. However, no subsequent researches were continued, which indicates there is still a long way to go for Mg-RE alloys.

4.2.3. Rheo-forming of MG-RE alloys

Rheo-forming, for instances the rheo-die casting and rheo-squeeze casting, is a one-step process along with the successfully prepared semisolid slurries, which utilizes the specially designed mold and equipment to process the slurries. The semisolid slurries preparation processes prior to rheo-forming can be variant among those aforementioned techniques.

Fang et al. [102] combined direct ultrasonic vibration with squeeze casting to fabricate the rheo-squeeze cast Mg-3RE-1Zn-1.4Y alloy, where the optical micrographs under various applied pressures were shown in Fig. 22). It was found that the tensile strengths of rheo-squeeze cast Mg-RE alloy was continuously increased with increasing the applied pressure from 0 MPa to 200 MPa. The YS, UTS and EL. of the alloy solidified under applied pressure of 200 MPa was 110 MPa, 180 MPa and 8.6%, respectively, which showed 17%, 19%, and 87% improvement than the alloy solidified without pressure. Chen et al. [111,112] combined electromagnetic stirring fabrication of the slurries with direct rheo-squeeze casting to process the Mg-Nd-Zn-Zr series alloys.

5. Applications of MG-RE alloys

From World War II to 1970s, Mg alloys had widely been used in aircrafts, bombers and missiles. At that time, the consumptions of flights and weapons were quick and the service time was not too long, and the inverse effect of poor corrosion resistance was not well performed. When it came to the 1980s, the wide applications of Mg alloys were restricted severely due to the systematic understanding of the poor mechanical performance in flammability, corrosion resistance, fatigue life and creep resistance, as well as the development of high-performance Al alloys. Until the late 1990s, the new series of Mg-RE alloy had been developed with certain ignition proof ability of melting without protecting atmosphere, good age-hardening response and excellent creep resistance that could work at as high as 350 °C.

5.1. Applications in aerospace and aviation industries

Until recently, in 2015, the Society of Automotive Engineers (SAE) has finally revised its statement of "*Magnesium alloys shall not be used*" to "*Magnesium alloys may be used in aircraft seat construction provided they are tested to and meet the flammability performance requirements in the FAA Fire Safety Branch document: Aircraft Materials Fire Test Handbook – DOT/FAA/AR-00/12, Chapter 25, Oil Burner Flammability Test for Magnesium Alloy Seat Structure*.". The Mg-RE series alloys, for instance, commercial Elektron® 43 (WE43C) and Electron® 21 (Mg-3Nd-1Gd-0.4Zn-0.5Zr), are firstly been accepted for applications in jet engines and military aircrafts. The Elektron® 43 then are able to be used as aircraft seats (Fig. 23) [113]. The Pratt & Whitney PW-100/150 series and PT-6 engines have been reported to use the Electron® 43 in integrated reduction gearboxes and other structural components [114,115]. In China, the development and application of Mg-RE alloys grow much faster in recent years due to the abundant reserves of Mg and RE resources. The government has allowed the application of Mg-RE parts or components to be assembled in helicopter and satellite, as shown in Fig. 24 [116].

5.2. Applications in weapon and defense industries

The Magnesium Elektron company has reported [113] that the developed Electron® 21 has gain applications in military helicopters to achieve higher horsepower at higher temperatures, for instance the Sikorsky H-60 series (Black Hawk, Seahawk and Special Forces versions), CH-47 Chinook, AH-64 Apache.

The application of Mg-RE alloys in weapon and defense industries in China has gain more attentions than other countries. The self-developed JDM1 (Mg-3Nd-0.2Zn-0.4Zr) [117] and JDM2 (Mg-10Gd-3Y-0.5Zr) [5] Mg-RE alloys by researchers in Shanghai Jiao Tong University have been enrolled in certain type of weapons, for instance, the light missiles (as shown in Fig. 25(a) ∼(c)) and some radar components (Fig. 25(d)∼(g)).

5.3. Applications in auto industry and other civil industries

As indicated in Section 4.3, the limited trials made in die cast Mg-RE has restricted the application of Mg-RE alloys

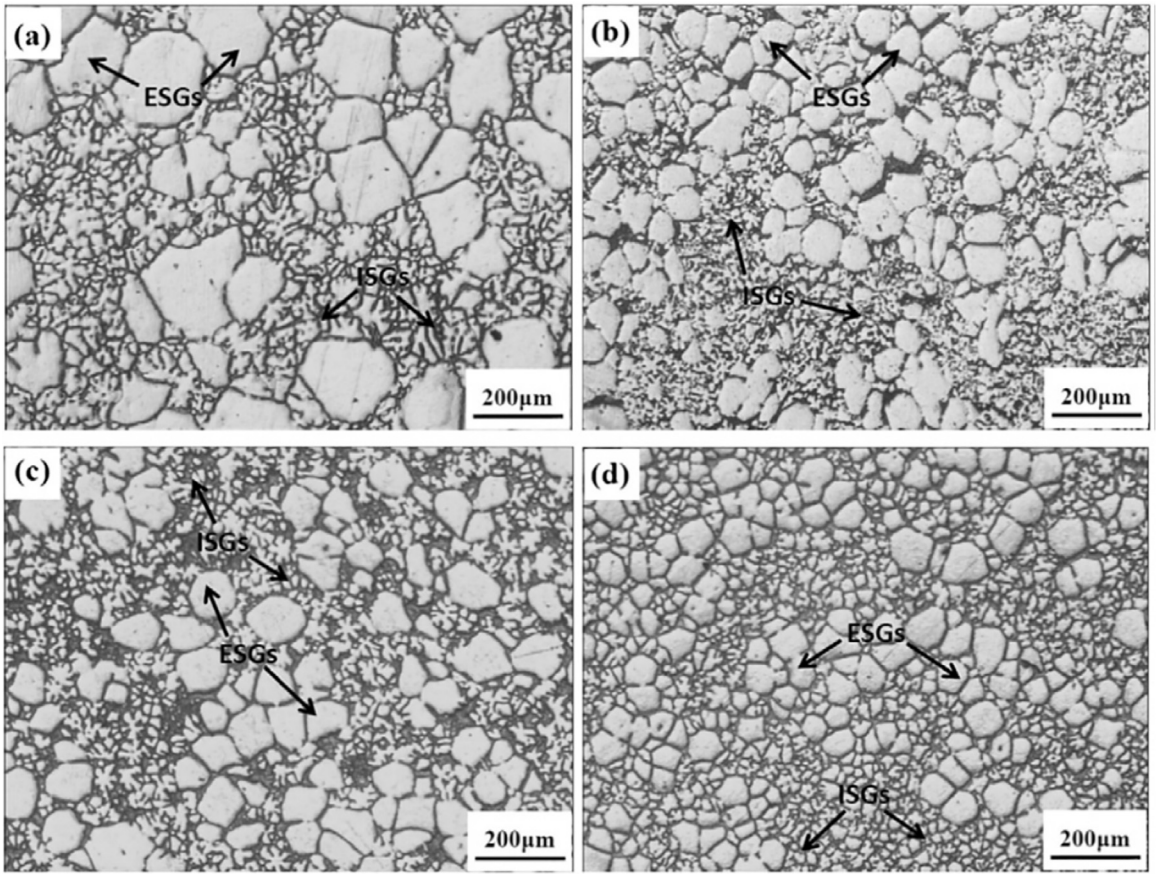

Fig. 22. Optical micrographs of rheo-squeeze cast Mg–3RE–6Zn–1.4Y alloys under different applied pressures: (a) 0 MPa, (b) 50 MPa, (c) 150 MPa, and (d) 200 MPa. The labeled ESGs in the figures are stands for external solidified grains [102].

Fig. 23. Airline seats made by Elektron® 43 magnesium alloy [113].

in the auto industry, due to the entrapped gas and porosities. In pursue of weight reduction in auto industry, there is a generally accepted approach to substitute Al with Mg casting components. The trials were executed by collaborations between several auto suppliers and research institutes in China. The V6 engine blocks head made of aforementioned JDM1 alloy was successfully fabricated by the low pressure sand cast process [118] (Fig. 26(a)). Subsequently, the engine cylinder head was manufactured by the similar Mg-RE alloy through tile-pouring technique (Fig. 26(c)). The engine cylinder head was installed to a car for road tests and found no wear occurred in the camshaft and tappet after undergoes 9000 km working [119]. Due to the relatively good casting ability and ductility, the JDM1 alloy was also prepared by composite fabrication methods of low pressure die cast plus flow forming (cast & flow forming) technology for car wheels [119] (Fig. 26(b)). Note that the microstructure of the alloy was refined through the flow forming process, and thus improved the mechanical properties of Mg-RE alloys (The YS, UTS and E_f were improved from 85 MPa, 138 MPa, and 4.8%, respectively in as-cast condition to 278 MPa, 317 MPa, and 8.4%, respectively after flow forming). The heat resistant Mg-Gd-Y alloy has been employed to fabricate piston components through squeeze casting technique, and showed a long term service ability at temperature as high as 300 °C [120].

6. Future prospects of high-performance MG-RE alloys

In review of the current progresses of the Mg-RE alloys and related technologies, there is still great steps needed for better development of the Mg-RE alloys. The urgent needs for higher strength and lighter weight components in

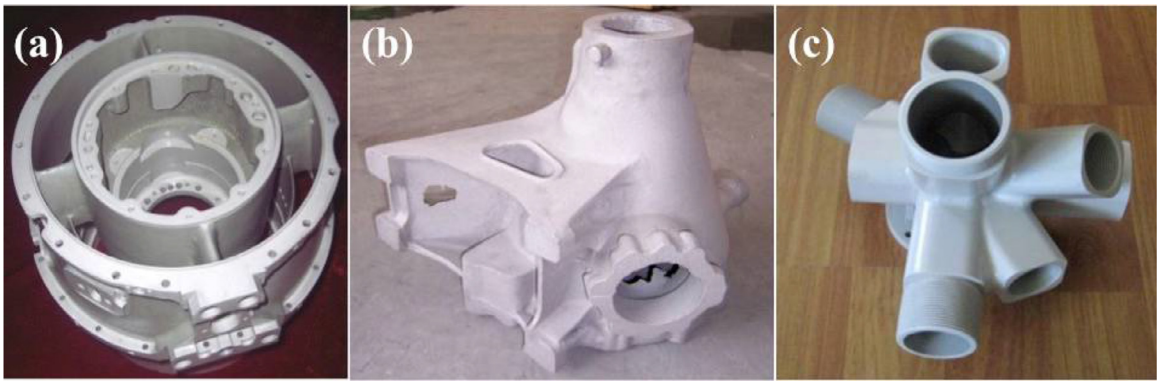

Fig. 24. Typical Mg-RE casting components: (a) Intermediate case of missile engine, (b) helicopter gearbox case, and (c) Satellite support component [116].

Fig. 25. Light missile shell (a ∼ c) prepared by JDM2 Mg-RE alloy and radar components (d ∼ g) [116].

engineering practice have urged the design of next generation Mg-RE alloys. The solutions may include obtaining fine and dense non-basal precipitates to create strong age-hardening responses and reducing the use of high-density solute elements. Since Mg-RE alloys are mainly towards elevated temperature applications, the grain refinement of Mg-RE alloys should consider the balance between room temperature strength and elevated temperature creep resistance, which also generates the design of strong grain boundaries to improve the creep resistance as the grain size was refined. Although

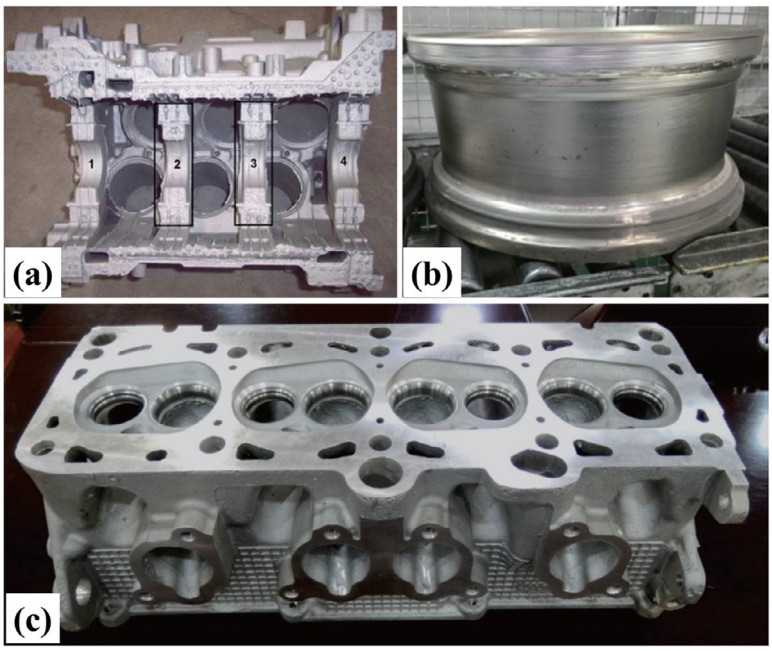

Fig. 26. Examples for application of Mg-RE alloys in auto industries: (a) V6 engine blocks of both alloys were cast in sand molds using a low pressure casting process [118], (b) 20-inch car wheel prepared by cast & flow forming technique [119], and (c) engine cylinder head made through tile-pouring method [119].

the melt purification of Mg-RE melts is solved in some cases, it is still a problem when incorporated with new casting technologies. More importantly, the newly developed casting technologies for Mg-RE should be widely promoted from research labs to enterprises, and the corresponding equipment and production line should be updated or redesigned for the new techniques. Finally, the engineering application of Mg-RE alloys should be further promoted to auto industry and other civil areas, which can in turn stimulate a better development of the alloys and related technologies.

To the authors understanding, the future research and development of cast Mg-RE alloy may focus on and may not limited to the following categories: (1) Alloy design and microstructural regulation of new generation cast Mg-RE alloys. The alloys should possess high strength, high ductility, good heat resistance and corrosion resistance, and with good castability. (2) New technologies and corresponded equipment for deep purification, compound grain refinement, and smelt protection of Mg-RE alloy melts. (3) The shape controlling, properties controlling and weld repairing of Mg-RE alloy casting with large dimension and complex structures. (4) Building of series material standards for new generation cast Mg-RE alloys.

7. Summary

The present study reviewed the current developments of high-performance cast Mg-RE alloys, especially on alloy design, melt purification, grain refinement techniques and castability, precision liquid processing and semisolid forming techniques, and engineering applications. The following conclusions can be made:

(1) Various systems of high strength Mg-RE alloys with strong age hardening response have been developed, whose combined properties strongly depend on the precipitates distribution of both basal and prismatic habit planes, and LPSO in certain case. The developed Mg-10Gd-3Y-0.5Zr alloy show overall promising high strength with moderate ductility strengthened by dense distribution of meta-stable β' phase, Mg-3Nd-0.2Zn-0.4Zr alloy with moderate strength while higher ductility due to the relatively low amount of alloying elements, and Mg-15Gd-1Zn-0.4Zr and Mg-11Y-5Gd-2Zn-0.5Zr alloys show better creep resistance that could be used at 300 °C due to the combined strengthening of β' and LPSO phases.

(2) The newly developed RE containing fluxes showed applicability to the Mg-RE alloy melt, and complex purification methods need more investigations. Mg-Zr mater alloys is still most effective grain refiners for Mg-RE alloys, while in-situ formed Al_2RE particles via addition of pure Al are applicable to certain types of Mg-RE alloys under certain casting solidification conditions. The fluidity and hot tearing susceptibility are better than conventional Mg-Al alloys due to the promising grain refining effect of Zr in Mg-RE alloys.

(3) Various casting techniques have been tried in Mg-RE alloys, during which process parameters control is important. Vacuum assisted high pressure die casting ensures the Mg-RE alloys a certain extent of heat treatment. Squeeze casting is promising to produce Mg-RE components with high strength. Several new slurry preparation and combined semisolid forming technologies were employed for Mg-RE alloys production, including direct ultrasonic or low frequency electro-magnetic assisted rheo-forming and isothermal holding assisted thixo-forming.

(4) In consideration of the special value of RE, high performance Mg-RE alloys have been successfully applied to several key areas such as aerospace and aviation industries, defense and weapon industries and auto industry. It is also expected that the use of Mg-RE alloys in such key areas will be in continuous growth.

Acknowledgements

This work is supported by the National Natural Science Foundation of China (Grant Nos. 51775334, 51821001 and 51701124), National Key Research and Development Program of China (Grant No. 2016YFB0701205), China Postdoctoral Science Foundation (Grant No. 2020M671360), Natural Science Foundation for Young of Jiangsu Province (Grant No. BK20190863), Jiangsu "Mass Innovation and Entrepreneurship" Talent Program (Shuang Chuang Ph.Ds, 2018), and Open Research Fund of the State Key Laboratory of Metal Matrix Composites (Grant No. sklmmc-kf18-08).

References

[1] L.L. Rokhlin, Magnesium alloys containing rare earth metals: structure and properties, Taylor & Francis, 2003.
[2] J. Zhang, S. Liu, R. Wu, L. Hou, M. Zhang, Journal of Magnesium and Alloys 6 (2018) 277–291.
[3] J. Davis, ASM Specialty Handbook: Aluminum and Aluminum Alloys, ASM International, Ohio, USA, 1993.
[4] M.M. Avedesian, H. Baker, ASM Specialty Handbook: Magnesium and Magnesium Alloys, ASM international, Ohio, USA, 1999.
[5] S. He, Shanghai Jiao Tong University, 2007.
[6] X.B. Liu, R.S. Chen, E.H. Han, J. Alloy. Compd. 465 (2008) 232–238.
[7] J. Wang, J. Meng, D. Zhang, D. Tang, Mater. Sci. Eng. A 456 (2007) 78–84.
[8] J.-l. Li, R.-s. Chen, W. Ke, Trans. Nonferrous Met. Soc. China 21 (2011) 761–766.
[9] C. Wang, G. Wu, E.J. Lavernia, W. Ding, J. Mater. Sci. 52 (2017) 1831–1846.
[10] J. Dai, S. Zhu, M.A. Easton, M. Zhang, D. Qiu, G. Wu, W. Liu, W. Ding, Mater. Sci. Eng. A 576 (2013) 298–305.
[11] N. Liu, Z. Zhang, L. Peng, W. Ding, Mater. Sci. Eng. A 627 (2015) 223–229.
[12] Z. Zhang, Shanghai Jiao Tong University, 2009.
[13] K. Zheng, Shanghai Jiao Tong University, 2008.
[14] D.-j. Li, X.-q. Zeng, J. Dong, C.-q. Zhai, Trans. Nonferrous Met. Soc. China 18 (2008) s117–s121.
[15] T. Ozaki, Y. Kuroki, K. Yamada, H. Hoshikawa, S. Kamado, Y. Kojima, Mater. Trans. 49 (2008) 2185–2189.
[16] S. Zhang, W.C. Liu, X.Y. Gu, C. Lu, G.Y. Yuan, W.J. Ding, J. Alloy. Compd. 557 (2013) 91–97.
[17] J. Zhang, Z. Leng, S. Liu, J. Li, M. Zhang, R. Wu, J. Alloy. Compd. 509 (2011) 7717–7722.
[18] Z. He, L. Peng, P. Fu, Y. Wang, X. Hu, W. Ding, Mater. Sci. Eng. A 604 (2014) 78–85.
[19] J. Li, Z. He, P. Fu, Y. Wu, L. Peng, W. Ding, Mater. Sci. Eng. A 651 (2016) 745–752.
[20] W. Rong, Y. Wu, Y. Zhang, M. Sun, J. Chen, L. Peng, W. Ding, Materials Characterization 126 (2017) 1–9.
[21] K. Yamada, H. Hoshikawa, S. Maki, T. Ozaki, Y. Kuroki, S. Kamado, Y. Kojima, Scripta Mater. 61 (2009) 636–639.
[22] Q. Wang, J. Chen, Z. Zhao, S. He, Mater. Sci. Eng. A 528 (2010) 323–328.
[23] Y. Zhang, Y. Wu, L. Peng, P. Fu, F. Huang, W. Ding, J. Alloy. Compd. 615 (2014) 703–711.
[24] J.-F. Nie, Metall. Mater. Trans. A 43 (2012) 3891–3939.
[25] X. Liu, Z.Q. Zhang, Q.C. Le, L. Bao, Journal of Magnesium and Alloys 4 (2016) 214–219.
[26] Q.Z. Liu, X.F. Ding, Y.P. Liu, X.J. Wei, J. Alloy. Compd. 690 (2017) 961–965.
[27] S.-y. Li, D.-j. Li, X.-q. Zeng, W.-j. Ding, Trans. Nonferrous Met. Soc. China 24 (2014) 3769–3776.
[28] A. Luo, M.O. Pekguleryuz, J. Mater. Sci. 29 (1994) 5259–5271.
[29] F. Penghuai, P. Liming, J. Haiyan, Z. Zhenyan, Z. Chunquan, Mater. Sci. Eng. A 486 (2008) 572–579.
[30] D. Li, Q. Wang, W. Ding, Mater. Sci. Eng. A 448 (2007) 165–170.
[31] Q. Zhang, Q.N. Li, X.T. Jing, X.Y. Zhang, Journal of Rare Earths 28 (2010) 375–377.
[32] Z. Liu, G. Wu, W. Liu, S. Pang, W. Ding, Mater. Sci. Eng. A 561 (2013) 303–311.
[33] H. Zhang, L. Zhang, G. Wu, A. Chen, W. Cui, Y. Chen, Q. Wang, Z. Gao, J. Mater. Res. 32 (2017) 3191–3201.
[34] H. Zhang, J. Fan, L. Zhang, G. Wu, W. Liu, W. Cui, S. Feng, Mater. Sci. Eng. A 677 (2016) 411–420.
[35] Z.J. Su, C.M. Liu, Y.C. Wan, Mater. Des. 45 (2013) 466–472.
[36] J.E. Saal, C. Wolverton, Acta Mater. 68 (2014) 325–338.
[37] X.H. Shao, Z.Q. Yang, X.L. Ma, Acta Mater. 58 (2010) 4760–4771.
[38] D.D. Yin, Q.D. Wang, Y. Gao, C.J. Chen, J. Zheng, J. Alloy. Compd. 509 (2011) 1696–1704.
[39] H.E. Friedrich, B.L. Mordike, Magnesium Technology: Metallurgy, Design Data, Applications, Springer Verlag, Berlin Heidelberg, 2006.
[40] Y.L. Li, G.H. Wu, A.T. Chen, W.C. Liu, Y.X. Wang, L. Zhang, J Mater Sci Technol 33 (2017) 558–566.
[41] Y.L. Li, G.H. Wu, W.C. Liu, A.T. Chen, L. Zhang, Y.X. Wang, China Foundry 14 (2017) 128–137.
[42] H. Huang, Y.X. Wang, P.H. Fu, L.M. Peng, H.Y. Jiang, W.Y. Xu, Int. J. Cast. Metals Res. 26 (2013) 213–219.
[43] Y. Huang, in: Shanghai Jiaotong University, Shanghai, 2009.
[44] J. Song, F. Pan, B. Jiang, A. Atrens, M.-X. Zhang, Y. Lu, Journal of Magnesium and Alloys 4 (2016) 151–172.
[45] W. Wang, G. Wu, Q. Wang, Y. Huang, W. Ding, Mater. Sci. Eng. A 507 (2009) 207–214.
[46] F. Pan, X. Chen, T. Yan, T. Liu, J. Mao, W. Luo, Q. Wang, J. Peng, A. Tang, B. Jiang, Journal of Magnesium and Alloys 4 (2016) 8–14.
[47] L.F. Zhang, T. Dupont, Materials Science Forum 546-549 (2007) 25–36.
[48] H. Cao, M. Huang, C. Wang, S. Long, J. Zha, G. You, Journal of Magnesium and Alloys 7 (2019) 370–380.
[49] W. Wei, W. Guohua, S. Ming, H. Yuguang, W. Qudong, D. Wenjiang, Mater. Sci. Eng. A 527 (2010) 1510–1515.
[50] X.G. Shujun Ji, Jianxiong Dong, Peng Su, China's Refractories 19 (2010) 8.
[51] J. Mei, W. Liu, G. Wu, L. Xiao, W. Ding, J. Mater. Res. 30 (2014) 224–232.
[52] J. Mei, W.-c. Liu, G.-h. Wu, Y. Zhang, Y.-t. Zhang, Y.-k. Hong, R.-x. Zhang, L. Xiao, W.-j. Ding, Trans. Nonferrous Met. Soc. China 25 (2015) 1811–1821.
[53] Y.C. Lee, A.K. Dahle, D.H. StJohn, Metall. Mater. Trans. A 31 (2000) 2895–2906.
[54] E. Karakulak, Journal of Magnesium and Alloys (2019).
[55] P. Saha, K. Lolies, S. Viswanathan, R. Batson, A. Gokhale, Magnesium Technology 2010 (2010).
[56] H. Okamoto, Phase diagrams of dilute binary alloys, ASM international, Ohio, USA, 2002.
[57] M. Qian, D.H. Stjohn, Int. J. Cast. Metals Res. 22 (2009) 256–259.
[58] S. Pang, G. Wu, W. Liu, M. Sun, Y. Zhang, Z. Liu, W. Ding, Mater. Sci. Eng. A 562 (2013) 152–160.
[59] S. Pang, G.H. Wu, W.C. Liu, L. Zhang, Y. Zhang, H. Conrad, W.J. Ding, Trans. Nonferrous Met. Soc. China 25 (2015) 363–374.
[60] S. Pang, G.H. Wu, W.C. Liu, L. Zhang, Y. Zhang, H. Conrad, W.J. Ding, Trans. Nonferrous Met. Soc. China 24 (2014) 3413–3420.
[61] J.L. Li, R.S. Chen, Y.Q. Ma, W. Ke, Thermochimica Acta 590 (2014) 232–241.

[62] M. Sun, D.H. StJohn, M.A. Easton, K. Wang, J.M. Ni, Metall. Mater. Trans. A 51 (2020) 482–496.
[63] M. Qian, L. Zheng, D. Graham, M.T. Frost, D.H. StJohn, Journal of Light Metals 1 (2001) 157–165.
[64] M. Sun, M.A. Easton, D.H. StJohn, G. Wu, T.B. Abbott, W. Ding, Adv. Eng. Mater. 15 (2013) 373–378.
[65] S. Ming, W. Guohua, D. Jichun, W. Wei, D. Wenjiang, J. Alloy. Compd. 494 (2010) 426–433.
[66] D. Qiu, M.X. Zhang, J.A. Taylor, P.M. Kelly, Acta Mater. 57 (2009) 3052–3059.
[67] J. Dai, M. Easton, M. Zhang, D. Qiu, X. Xiong, W. Liu, G. Wu, Metall. Mater. Trans. A 45 (2014) 4665–4678.
[68] C. Wang, J. Dai, W. Liu, L. Zhang, G. Wu, J. Alloy. Compd. 620 (2015) 172–179.
[69] Z. Jiang, B. Jiang, Y. Zeng, J. Dai, F. Pan, Mater. Sci. Eng. A 645 (2015) 57–64.
[70] Y.L. Li, G.H. Wu, A.T. Chen, H.R.J. Nodooshan, W.C. Liu, Y.X. Wang, W.J. Ding, J. Mater. Res. 30 (2015) 3461–3473.
[71] B. Zhou, D. Wu, R. Chen, E.-H. Han, Adv. Eng. Mater. (2019).
[72] P.H. Fu, A.A. Luo, H.Y. Jiang, L.M. Peng, Y.D. Yu, C.Q. Zhai, A.K. Sachdev, J. Mate. Process. Technol. 205 (2008) 224–234.
[73] W. Qilong, G. Wu, Z. Hou, B. Chen, Y. Zheng, W. Ding, China Foundry 7 (2010) 6–12.
[74] L. CAO, W.-c. LIU, Z.-q. LI, G.-h. WU, L. XIAO, S.-h. WANG, W.-j. DING, Trans. Nonferrous Met. Soc. China 24 (2014) 611–618.
[75] W.C. Liu, B.P. Zhou, G.H. Wu, L. Zhang, X. Peng, L. Cao, Journal of Magnesium and Alloys 7 (2019) 597–604.
[76] J.M. Mao, W.C. Liu, Y.L. Li, G.L. Wei, L. Zhang, W.B. Zou, Y. Tian, G.H. Wu, J. Mater. Res. 31 (2016) 2538–2548.
[77] L.M. Peng, P.H. Fu, Z.M. Li, Y.X. Wang, H.Y. Jiang, J. Mater. Sci. 49 (2014) 7105–7115.
[78] Z.J. Liu, G.H. Wu, W.C. Liu, S. Pang, W.J. Ding, Mater. Sci. Eng. A 561 (2013) 303–311.
[79] Z.J. Liu, G.H. Wu, W.C. Liu, S. Pang, W.J. Ding, Trans. Nonferrous Met. Soc. China 22 (2012) 1540–1548.
[80] J.P. Weiler, Journal of Magnesium and Alloys 7 (2019) 297–304.
[81] S. Zhu, M.A. Easton, T.B. Abbott, M.A. Gibson, J.-F. Nie, Adv. Eng. Mater. 18 (2016) 932–937.
[82] Q. Peng, L. Wang, Y. Wu, L. Wang, J. Alloy. Compd. 469 (2009) 587–592.
[83] S. Gavras, S.M. Zhu, J.F. Nie, M.A. Gibson, M.A. Easton, Mater. Sci. Eng. A 675 (2016) 65–75.
[84] Y. Zhou, Z. Guo, S.M. Xiong, J. Mate. Process. Technol. 267 (2019) 366–375.
[85] X. Dong, X. Zhu, S. Ji, J. Mate. Process. Technol. 266 (2019) 105–113.
[86] M.R. Ghomashchi, A. Vikhrov, J. Mate. Process. Technol. 101 (2000) 1–9.
[87] H. Hu, J. Mater. Sci. 33 (1998) 1579–1589.
[88] S.Z. Wang, Z.S. Ji, S. Sugiyama, J. Yanagimoto, Adv Mech Eng 2014 (2014).
[89] Y. Gan, D. Zhang, W. Zhang, Y. Li, Int. J. Cast. Metals Res. 28 (2015) 50–58.
[90] N. Souissi, S. Souissi, C. Niniven, M. Amar, C. Bradai, F. Elhalouani, Metals 4 (2014) 141–154.
[91] B. Lin, W.W. Zhang, Z.H. Lou, D.T. Zhang, Y.Y. Li, Mater. Des. 59 (2014) 10–18.
[92] S.B. Bin, S.M. Xing, L.M. Tian, N. Zhao, L. Li, Trans. Nonferrous Met. Soc. China 23 (2013) 977–982.
[93] K.M.A. Haider, N.A. Mufti, JOM 66 (2014) 1446–1453.
[94] S. Xu, C.H.M. Simha, M. Gesing, J. Liang, J. Lo, Journal of Magnesium and Alloys 3 (2015) 188–196.
[95] W.F. Mo, L. Zhang, G.H. Wu, Y. Zhang, W.C. Liu, C.L. Wang, Mater. Des. 63 (2014) 729–737.
[96] Y. Yanling, P. Liming, F. Penghuai, H. Bin, D. Wenjiang, Y. Baozheng, Mater. Trans. 50 (2009) 2820–28252825.
[97] C. Wang, E.J. Lavernia, G. Wu, W. Liu, W. Ding, Metall. Mater. Trans. A 47 (2016) 4104–4115.
[98] Q. Zhao, Y. Wu, W. Rong, K. Wang, L. Yuan, X. Heng, L. Peng, Journal of Magnesium and Alloys 6 (2018) 197–204.
[99] J. Sun, L. Zhang, G. Wu, W. Liu, Z. Hu, A. Chen, J. Mate, Process. Technol. 225 (2015) 485–491.
[100] X. Fang, S. Wu, S. Lü, J. Wang, X. Yang, Mater. Sci. Eng. A 679 (2017) 372–378.
[101] S.L. Lu, X. Yang, L.Y. Hao, S.S. Wu, X.G. Fang, J. Wang, Met. Mater. Int. 24 (2018) 1315–1326.
[102] X. Fang, S. Lü, L. Zhao, J. Wang, L. Liu, S. Wu, Mater. Des. 94 (2016) 353–359.
[103] C. Wang, A. Chen, L. Zhang, W. Liu, G. Wu, W. Ding, Mater. Des. 84 (2015) 53–63.
[104] C. Wang, G. Wu, M. Sun, L. Zhang, W. Liu, W. Ding, J. Mate. Process. Technol. 279 (2020) 116545.
[105] Y. Chen, L. Zhang, W. Liu, G. Wu, W. Ding, Mater. Des. 95 (2016) 398–409.
[106] G. Wu, Y. Zhang, W. Liu, W. Ding, Journal of Magnesium and Alloys 1 (2013) 39–46.
[107] G. Chen, S. Zhang, H. Zhang, F. Han, G. Wang, Q. Chen, Z. Zhao, J. Mate. Process. Technol. 259 (2018) 88–95.
[108] Y. Meng, Q. Chen, S. Sugiyama, J. Yanagimoto, J. Mate. Process. Technol. 247 (2017) 192–203.
[109] Y. Meng, Q. Li, Y. Tang, S. Sugiyama, Vacuum 150 (2018) 173–185.
[110] Z.Y. Xie, Y. Tian, Q. Li, J.C. Zhou, Y. Meng, Int J Adv Manuf Tech 101 (2019) 1807–1819.
[111] Y. Chen, G. Wu, W. Liu, L. Zhang, S. Zhang, J. Mater. Res. 33 (2018) 758–771.
[112] Y. Chen, G. Wu, W. Liu, L. Zhang, Q. Wang, J. Mater. Res. 32 (2017) 4206–4218.
[113] Website of Magnesium Elektron: https://www.magnesium-elektron.com/markets/aerospace, access date: Mar. 3rd, 2020
[114] A.A. Luo, Journal of Magnesium and Alloys 1 (2013) 2–22.
[115] G. Wardlow, in: Presentation at the 64th Annual World Magnesium Conference, Vancouver, BC, Canada, 2007 May 13the15th.
[116] G. Wu, Y. Chen, W. Ding, Manned Spaceflight 22 (2016) 12.
[117] F. Penghuai, P. Liming, J. Haiyan, C. Jianwei, Z. Chunquan, Mater. Sci. Eng. A 486 (2008) 183–192.
[118] Z.M. Li, Q.G. Wang, A.A. Luo, L.M. Peng, P.H. Fu, Y.X. Wang, Mater. Sci. Eng. A 582 (2013) 170–177.
[119] P. Fu, L. Peng, W. Ding, Strategic Study of Chinese Academy of Engineering (2018) 84–90.
[120] J. Yuan, Q.D. Wang, D.D. Yin, H. Wang, C.J. Chen, B. Ye, Materials Characterization 78 (2013) 37–46.